Baiting Proteins with C_{60}

Matteo Calvaresi* and Francesco Zerbetto*

Dipartimento di Chimica "G. Ciamician", Universita' di Bologna, V. F. Selmi 2, 40126 Bologna, Italy

ARTICLE

ABSTRACT About 20 proteins are known to modify their activity upon interaction with C_{60}. Their structures are present in a database that includes more than 1200 protein structures selected as possible targets for drugs and to represent the entire Protein Data Bank. The set was examined with an algorithm that appraises quantitatively the interaction of C_{60} and the surface of each protein. The redundancy of the set allows to establish the predictive power of the approach that finds explicitly the most probable site where C_{60} docks on each protein. About 80% of the known fullerene binding proteins fall in the top 10% of scorers. The close match between the model and experiments vouches for the accuracy of the model and validates its predictions. The sites of docking are shown and discussed in view of the existing experimental data available for protein—C_{60} interaction. A closer exam of the 10 top scorers is discussed in detail. New proteins that can interact with C_{60} are identified and discussed for possible future applications as drug targets and fullerene derivatives bioconjugate materials.

KEYWORDS: fullerene · proteins · bioconjugate · drug design · nanotoxicology

INTRODUCTION

Over the last two decades, there has been considerable effort devoted to understanding the interactions between the *all-carbon* nanotubes and fullerenes with biological molecules.[1] The development of these hybrid materials was intended to drive advancement in nanoscience, biochemistry,[2] and materials chemistry.[3] Information on the interactions between C_{60} and proteins can help explaining its pharmacological activity and also provide indications about its potential toxicity, a topic still under debate.[4,5] Examples of fullerene and fullerene derivative bioactivities are well-known and include antibacterial activity,[6] neuroprotection,[7,8] DNA cleavage,[9] apoptosis,[10] ion channel inhibition,[11] and amyloid formation inhibition.[12] Enzyme inhibition by fullerene-based compounds was found, among the rest, for nitric oxide synthases,[13] glutathione reductase,[14] cysteinic proteases (papaine, cathepsine), and serinic proteases (tripsine, plasmine, thrombin).[15] Antiviral activity of fullerenes was demonstrated in the inhibition of HIV protease, initially by modeling and subsequently by *in vitro* studies.[16−19] Interactions of fullerenes with other proteins were also documented, including a fullerene-specific antibody,[20,21] human serum albumin, HSA, bovine serum albumin, BSA,[22−24] and lysozyme.[25]

The conjugate materials have enhanced solubilization[26] and cellular delivery properties.[27] They have been used for the development of new sorting and purification techniques,[28] in biomedical[29] and electronic devices,[30] and appear promising for developing novel chemical[31] and biological[32] sensing instruments, as well as for controlling binding and assembly onto templating surfaces.[33,34]

It is fair to say that to date understanding of fullerene−protein interactions has only been partly achieved and much remains to be done when it comes to prediction. The reason mainly lies in the fact that we know relatively few proteins that interact or can interact with the fullerene cage. No systematic study has been carried out to identify fullerene-binding proteins and every new discovery was guided by chemical intuition, scientific curiosity, and, ultimately, by serendipity.

The intent of this work is to lay the ground for a systematic computational approach able to account for such interactions. The investigation of the interface between biosystems and materials poses some serious difficulties both experimentally[33,35] and to simulations,[36,37] because it is often at the boundary between different scientific communities and distinctly different approaches. It also offers the opportunity to merge models and information that have been collected independently. Typical techniques to investigate biosystems are database screening and docking,[38−41] techniques that have been

*Address correspondence to matteo.calvaresi@studio.unibo.it, francesco.zerbetto@unibo.it..

Received for review December 11, 2009 and accepted March 19, 2010.

Published online April 1, 2010.
10.1021/nn901809b

of help in drug design. The docking of C_{60} with proteins is potentially simple to describe, if compared to the docking of common molecules, especially if the structures are maintained rigid. Very recently the predictive ability of docking algorithms was demonstrated on the search of the best fullerene that can bind a specific protein, namely, HIV-1 PR.[42,43] The reverse ligand-protein docking approach[44−46] identifies possible binding proteins for a specific molecule, namely, C_{60}, rather than binding molecules for a specific protein as in "direct" docking.

An important database of protein structures is the drug target database, PDTD,[47] a comprehensive, web-accessible database. PDTD contains 1207 entries that cover 841 known and potential drug targets with structures taken from the Protein Data Bank, PDB, and is representative of the entire PDB. Investigation of the interactions of C_{60} with all these proteins can reveal candidates for fullerene binding that can also be exploited in nanotechnology. It can also suggest for which diseases fullerene derivatives can be developed and tested as potential drugs or where they can be potentially toxic.

Fullerene Binding to Proteins: Guilty by Evidence. C_{60} discovery dates back to 1985.[48] Until 1993, there was a complete lack of data on the biological activity of C_{60}, because of its insolubility in aqueous solutions. With the availability of functionalized fullerenes, the first studies were started. In the following, we describe the temporal development of the investigations of the interactions between fullerene derivatives and biosystems.

HIV Protease. In 1993, Wudl, Friedman, and co-workers proposed, for the first time, fullerene as an HIV protease, HIVP, inhibitor.[16] On the basis of molecular modeling, they recognized that the C_{60} cage can be accommodated almost perfectly inside the active site of the enzyme. Their prediction was confirmed experimentally. Kinetic analysis of HIVP in the presence of a water-soluble C_{60} derivative suggested a competitive mode of inhibition, consistent with the predicted binding mode. The dissociation rates were around $10^{-6}-10^{-9}$ M and the inhibition constant was 5.3 μM.

Cysteine and Serine Proteinases. The preparation of water miscible fullerene carboxylic acid by Nakamura and Sugiura groups[15,49] allowed a preliminary exam of inhibitory activity against various enzymes. This fullerene derivative was found to have considerable activity against cysteine proteinases (*m*-calpain $IC_{50} = 3.6$ μM, cathepsin B $IC_{50} = 10.5$ μM, papain $IC_{50} = 43$ μM) and serine proteinases (trypsin $IC_{50} = 5.6$ μM, plasmin $IC_{50} = 3.2$ μM, thrombin 24% inhibition at 10 μM).

Glutathione S-Transferase and Reductase. A kinetic study,[50] using purified mouse glutathione S-transferase, GST, with ethacrynic acid (25−100 μM) as the substrate, revealed that C_{60} is a noncompetitive inhibitor of GST enzyme with a $K_i = 48.8 \pm 0.25$ μM. Glutathione reductase, GR, is instead effectively inhibited only by fullerene derivatives, which have a carboxylic acid moiety.[14]

After these initial studies, the investigation of the toxicity of C_{60} and related systems started in earnest. They provided a host of information about the interactions between these compounds and proteins.

Cytochrome P450. Addition of fullerenol to mouse liver microsomes suppresses monooxygenase activities of cytochrome P450 toward benzo[a]pyrene, 7-ethoxycoumarin, aniline, and erythromycin with IC_{50} values of 42, 94, 102, and 349 μM.[51] Fulleronol also exhibits noncompetitive and mixed type of inhibition in benzo[a]pyrene hydroxylation and 7-ethoxycoumarin O-de-ethylation of cytochrome P450.[51]

ATPase. Direct measurement of mitochondrial Mg^{2+}-ATPase activity showed that the enzyme was inhibited, concentration-dependently, by fullerenol with an IC_{50} value of $7.1 + 0.3$ μM.[51]

Tubulin. Studying the effect of $C_{60}(OH)_{24}$ on tubulin polymerization, it was discovered that fulleronol can inhibit tumor cell growth by blocking the microtubule assembly *in vitro*.[52] The finding implies that C_{60} interacts with microtubule proteins and that the rate and extension of microtubule formation can be influenced by C_{60} presence.

Antibody Fab Fragment. The mouse immune repertoire is diverse enough to recognize and produce antibodies specific for fullerenes. Erlanger and co-workers succeeded in isolating several monoclonal anti-C_{60} antibodies[20] and solved by X-ray crystallography the structure of one of them, namely, an anti-Buckminsterfullerene antibody Fab fragment.[21] Its structure is, however, not present in the PDTD database. Specificity for C_{60} was determined by competitive inhibition (affinity of the antibody-fullerene complex was 22 nM). A shape-complementary clustering of hydrophobic amino acids, several of which participate in putative stacking interactions with fullerene, forms the binding site. The induced fit mechanism responsible for the fullerene binding processmakes it unelegible for the screening of the next section.

Glutamate Receptors. Carboxy- and polyhydroxylated-fullerenes were identified as neuroprotective agents.[7] This ability was first believed to be due to their antioxidant properties, but it was then demonstrated that they can exert their neuroprotective functions by blocking glutamate receptors, GluR.[8] Fullerenols were found to inhibit GluR binding in a dose-dependent manner. The binding of [^{3}H]-Glu to GluR is inhibited to an extent of 10, 53, and 80% by fullerenols at 10, 50, and 100 μM concentrations. Among the ionotropic GluR, AMPA receptor was found to be most sensitive to fullerenols, being inhibited to about 90% by 100 μM fullerenols, followed by KA and NMDA receptors that are inhibited to about 73 and 54%.[8] These structures are not present in PDTD. In most cases, only segments of these membrane

proteins have been crystallized in very recent times and they will not be included in the further analysis.

Nitric Oxide Synthase. C_{60} derivatives inactivate selectively neuronal nitric oxide synthase isoforms, NOS. The inactivation is time-, fullerene concentration-, and turnover-dependent and is not reversible upon dilution. A diamine adduct of C_{60} shows an $IC_{50} = 2.5$ μM.[53]

Nitric Oxide Synthase and Troponin. Addition of rabbit skeletal muscle troponin C to the inactivated NOS can reverse the inhibition promoted by D3-trisamine fullerene, showing that troponin has a higher affinity toward this fullerene derivative.[13]

Ion Channels. C_{60} derivatives were identified as a novel class of biological membrane ion channel blockers.[11] Electrophysiological experiments were conducted on different pore-forming channel subunits heterologously expressed in mammalian CHO cells. C_{60} had a significant effect on channels formed by *Caenorhabditis elegans* EXP-2, KVS-1, human KCNQ1 and Kv4.2, as well as HERG potassium channels, but did not affect endogenous CHO cell ClC-3 channels.[11] Qualitatively, C_{60} acted to inhibit ion currents to different extents, with a higher susceptibility of KCNQ1 and HERG. HERG was then used as a representative example. Whole-cell HERG currents were recorded in the absence and in the presence of C_{60} in test solutions. Inhibition was reversible, and it was suggested that the interaction takes place in extracellular domains of the channel.

Serum Albumin. The preparation and characterization of a stable human serum albumin, HSA, complex with C_{60} was also reported.[22] To determine quantitatively the binding constant, a fluorescence titration study was carried out and a value of 1.2×10^7 M^{-1} was reported.[22] The value of the binding constant is comparable to that published for other organic molecules that strongly bind to the same site of HSA, such as bilirubin (9.5×10^7 M^{-1}), iodipamide (9.9×10^6 M^{-1}), and 3-carboxy-4-methyl-5-propyl-2-furanpropanoate (1.3×10^7 M^{-1}). Similar results were obtained with bovine serum albumin, BSA.[54] The UV−visible spectrum of the purified BSA-C_{60} hybrid revealed features belonging to both components and proved the binding.[54]

HIV-Reverse Transcriptase. Anti-HIV activity of fullerene has long been associated with C_{60} HIV-protease inhibition, but recently, a study demonstrated that also the activity of HIV-reverse transcriptase is affected by the presence of fullerenes.[55] Eight different fullerene derivatives were tested and gave IC_{50} values smaller than 1.7 μM. One of them showed an IC_{50} of 0.029 μM.[55] These results are important considering that all the fullerene derivatives examined are more effective than the nonnucleoside analog of the HIV-RT inhibitor, nevirapine ($IC_{50} = 3$ μM) that, under the brand name Viramume, is commonly used to treat HIV infection.

Acethylcholineaterase. Design of possible fullerene binding proteins led to test fullerene derivatives as inhibitors of acethylcholineaterase, AChE.[56] This enzyme contains a hydrophobic cavity with the ideal size to accommodate a fullerene moiety. Four cationic fulleropyrrolidinium ions were synthesized and their inhibitory activity was determined. It was demonstrated that they inhibit the enzymatic activity of acetylcholinesterase, that the inhibition process is noncompetitive, and that the values of the affinity constants are in the micromolar range (IC_{50} vary from 15.6 to 31.4 μM).[56] A typical value for competitive inhibitors of AChE, used also pharmaceutically, is that of edrophonium chloride, with $IC_{50} = 0.054$ μM.

Lysozyme. Lysozyme has also been widely used as a model protein in nonbiological contexts. Fluorescence spectroscopy revealed that fullerenol can specifically bind to hen egg white lysozyme, with an association constant of 1.3×10^5 M^{-1}.[25] Activity assay showed that, as the fullerenol concentration increases, the activity of lysozyme decreases significantly. When the molar ratio of fullerenol/lysozyme is 5:1 (16.6 μM of fullerenol), lysozyme forfeits half of its activity.[25]

Inhibiting Allergic Responses. Very recent studies discovered that fullerenes are capable of inhibiting allergic responses *in vitro* and *in vivo* and suggested that these molecules have previously unrecognized antiallergic properties.[57] Protein microarray demonstrated that inhibition involves profound reductions in the activation of signaling molecules involved in mediator release and oxidative stress. Some protein signaling was inhibited more than 100-fold and involves important proteins such as serine and tyrosine kinases, phosphoinositide-3-kinase, and progesterone receptor.[57]

RESULTS AND DISCUSSION

Database Screening. Screening of a protein database with a docking procedure can reveal potential fullerene binding targets of interest for biological and pharmacological activity.[58] These target proteins may also find application in the manipulation and supramolecular assembly of fullerenes and nanotubes. A reasonable threshold for the reliable prediction of good targets in the drug target database (PDTD) can be set by selecting the top 10% of the most binding proteins,[59] which forms a set of about 120 proteins.

Table 1 presents the 10% most binding proteins as ranked by the reverse docking program employed here. In the following, we try to analyze the results by a comparison with literature data of binding of C_{60} with proteins

Analysis of the Rank. Rank 1 is occupied by the voltage-gated potassium channel. C_{60} is an ion channel blocker[11] that hampers channel functioning by fitting into the pore and hindering ion movement. Electrophysiological experiments demonstrated that the inhibition is ineffective on endogenous ClC-3 channels. The ClC-3 channel is here ranked 799! The protocol strongly discriminates the different behavior of the two kinds of channels. The docking results shown in Figure 1 indi-

TABLE 1. Top 10% of the Protein Target Candidates for C_{60} Binding, Identified by Reverse Docking Procedure

rank	ID (PDB)	biochemical function	therapeutical area	target details
1	1JVM	ion channels		voltage-gated potassium channel
2	1NHZ	factor, regulator, and hormones, receptor		glucocorticoid-like receptor
3	1P93	factor, regulator, and hormones, receptor	hormones and hormone antagonists	glucocorticoid receptor
4	1ME8	enzyme	immunomodulation	inosine monophosphate dehydrogenase (*de novo* synthesis Of purines)
5	1JKX	enzyme	neoplastic diseases	glycinamide ribonucleotide formyltransferase
6	1C41	enzyme		lumazine synthase
7	1PS9	enzyme	renal and cardiovascular functions	2,4-dienoyl-CoA reductase
8	1DHJ	enzyme	immunomodulation, neoplastic diseases	dihydrofolate reductase
9	1ILH	nuclear receptor		pregnane X receptor
10	1J96	enzyme	hormones and hormone antagonists	aldo-keto reductase family 1 member C3
11	1ACJ	enzyme	neoplastic diseases	acetylcholinesterase
12	1US0	enzyme		aldose reductase
13	1E7S	enzyme		GDP-fucose synthetase
14	2BCE	enzyme		cholesterol esterase
15	1B74	enzyme		glutamate racemase
16	1MCS	monoclonal antibodies	immunomodulation	immunoglobulin λ light chain dimer (Mcg)
17	1DBB	monoclonal antibodies	immunomodulation	Fab′ fragment of the Db3 anti-steroid monoclonal antibody
18	3ERT	nuclear receptor	neoplastic diseases	estrogen receptor α
19	1PPI	enzyme	hormones and hormone antagonists	α-amylase
20	1KAE	enzyme	synaptic and neuroeffector junctional sites and central nervous system	histidinol dehydrogenase
21	2NSE	enzyme		nitric oxide synthase
22	1J99	enzyme	hormones and hormone antagonists	alcohol sulfotransferase
23	1DHT	enzyme	hormones and hormone antagonists	estrogenic 17-β hydroxysteroid dehydrogenase
24	1CJ0	enzyme	blood and blood-forming organs	serine hydroxymethyltransferase, mitochondrial
25	1CI7	enzyme	viral infections, fungal infections, neoplastic diseases, parasitic infectious diseases	Thymidylate Synthase
26	1W7L	enzyme		kynurenine oxoglutarate transaminase
27	1AEV	enzyme	hormones and hormone antagonists	peroxidase
28	1TCO	enzyme	immunomodulation	FKBP, tacrolimus binding protein, FK506 binding protein
29	1DTL	structural proteins	hormones and hormone antagonists, renal and cardiovascular functions	cardiac troponin C (ctnc), Troponin T, cardiac muscle isoforms
30	1DKF	receptor	hormones and hormone antagonists	retinoid X receptor
31	2F9Q	enzyme		cytochrome P450 2D6 (CYP2D6)
32	1OSV	nuclear receptor, receptor	gastrointestinal functions	farnesoid X receptor
33	1DIY	enzyme		prostaglandin H synthase-1
34	1ZZE	enzyme		carbonyl reductase
35	1M08	enzyme		ATPase
36	2CHT	enzyme		chorismate mutase
37	1UTR	binding protein		mammalian PCB-binding protein
38	1TYP	enzyme	parasitic infectious diseases	trypanothione reductase
39	9AAT	enzyme	vitamins	aspartate aminotransferase
40	1UPW	receptor		liver X receptor β
41	1GPB	enzyme	hormones and hormone antagonists	glycogen phosphorylase, muscle form
42	1CZ7	enzyme, factor, regulator, and hormones	fungal infections	microtubule protein
43	1HDC	enzyme	gastrointestinal functions, inflammation	3-α-hydroxysteroid dehydrogenase
44	1V7M	monoclonal antibodies		MGDF receptor
45	1AL8	enzyme		oxidase
46	1XAN	enzyme		glutathione reductase
47	1EFR	enzyme		bovine mitochondrial F1-ATPase
48	1ZID	enzyme		enoyl-[acyl-carrier-protein] reductase [NADH]
49	1IIC	enzyme		peptide *N*-myristoyltransferase
50	3BTO	enzyme	parasitic infectious diseases	alcohol Dehydrogenase
51	1IAY	enzyme		1-aminocyclopropane-1-carboxylate synthase 2
52	1ORD	enzyme	bacterial infections	ornithine decarboxylase
53	1OSZ	monoclonal antibodies		MHC class I H-2KB heavy chain
54	1O7D	enzyme		α-mannosidase
55	2LGS	enzyme		glutamine synthetase
56	1E7W	enzyme	neoplastic diseases	flavohemoglobin
57	2PLV	enzyme	viral infections	poliovirus (type 1, mahoney strain)
58	1CSB	enzyme		cathepsin B
59	1JR1	enzyme	immunomodulation	inosine-5′-monophosphate dehydrogenase 2, IMP-2 dehydrogenase

TABLE 1. Continued

rank	ID (PDB)	biochemical function	therapeutical area	target details
60	1W07	enzyme		acyl CoA oxidase-1
61	4PAH	enzyme		phenylalanine hydroxylase
62	1HJ1	nuclear receptor	hormones and hormone antagonists	estrogen receptor β
63	1FXO	enzyme		glucose phosphate thymidylyltransferase
64	1NM8	enzyme		carnitine acyltransferase
65	2BE1	enzyme		IRE1 protein kinase
66	1ZZD	enzyme		ribonucleotide reductase
67	1BBP		gastrointestinal functions	bilin binding protein
68	1Q0N	enzyme		HPPK
69	1TVR	enzyme	viral infections	HIV-1 reverse transcriptase
70	1CLY			murine BR96 Fab
71	2C6C	enzyme		glutamate carboxypeptidase II
72	1R31	enzyme		HMG CoA reductase
73	1YTV	receptor		vasopressin V1a receptor
74	1E8W	enzyme		phosphoinositide 3-kinase (PI3K)
75	1ITZ	enzyme	vitamins	phosphotransketolase
76	2C6Q	enzyme		GMP reductase
77	2DDH	enzyme		acyl CoA oxidase-2
78	1HHJ	enzyme	viral infections	human class I histocompatibility antigen
79	1JS3	enzyme	hormones and hormone antagonists	aromatic-L-amino acid decarboxylase
80	1LYW	enzyme		cathepsin D
81	2VAA	monoclonal antibodies		murine MHC class I H-2Kb
82	1GNX	enzyme	hormones and hormone antagonists	β-glucosidase
83	1B8P	enzyme		malate dehydrogenase
84	1BMQ	enzyme		interleukin-1 β converting enzyme (ICE)
85	2R07	enzyme	viral infections	rhinovirus 14 (HRV14)
86	1OXO	enzyme	synaptic and neuroeffector junctional sites	aspartate aminotransferase, cytoplasmic
87	1ACY	monoclonal antibodies		HIV-1 gp120 protein
88	7AAT	enzyme		mitochondrial complex I B9 subunit
89	1CR1	enzyme	neoplastic diseases	DNA primase/helicase
90	1H5U	enzyme		glycogen phosphorylase
91	1JBQ	enzyme	vitamins	cystathionine β-synthase, cystathionine synthase
92	1QQD	monoclonal antibodies, receptor		histocompatibility leukocyte antigen (Hla)-Cw4 (heavy chain)
93	1K4W	factor, regulator, and hormones	hormones and hormone antagonists	nuclear orphan receptor Lxr-β
94	1QPB	enzyme	vitamins	pyruvate decarboxylase
95	1P8V	enzyme	blood and blood-forming organs	thrombin
96	1NEK	enzyme		succinate dehydrogenase
97	1IGJ	monoclonal antibodies	immunomodulation	Fab (Igg2A)
98	1HKV	enzyme	bacterial infections	mycobacterium diaminopimelate decarboxylase
99	2MCP	monoclonal antibodies	immunomodulation	immunoglobulin McPC603 Fab-phosphocholine
100	1HRI	enzyme	viral infections	human rhinovirus 14
101	1R12	enzyme		ADP-ribosyl cyclase
102	1A4W	enzyme	blood and blood-forming organs	serine proteinase α-thrombin
103	1V8B	enzyme		adenosylhomocysteinase
104	1MRK	enzyme		α-trichosanthin
105	1EFA	nuclear receptor		Lac repressor
106	1I9C	enzyme	blood and blood-forming organs	glutamate mutase
107	1BYB	enzyme		β-amylase
108	1DGD	enzyme		dialkylglycine decarboxylase
109	6COX	enzyme	inflammation	cyclooxygenase 1,2 (COX-1, COX-2)
110	1SEZ	enzyme		protoporphyrinogen oxidase
111	2SIM	enzyme	viral infections	neuraminidase
112	1W6K	enzyme		oxidosqualene cyclase
113	1JH7	enzyme		cyclic nucleotide phosphodiesterase
114	1RNE	enzyme	renal and cardiovascular functions	renin
115	1PMT	enzyme		glutathione transferase
116	1FM6	receptor	hormones and hormone antagonists	peroxisome proliferator activated receptor γ (PPAR γ)
117	4CTS	enzyme		citrate synthase
118	1AID	enzyme	viral infections	HIV protease
119	1USH	enzyme		nucleotidase
120	1CQE	enzyme	inflammation	prostaglandin G/H synthase 1, COX- 1, prostaglandin H2 synthase-1, COX-1, prostaglandin H2 synthase-1, COX-1
121	1HDO	enzyme		biliverdin Ix β reductase

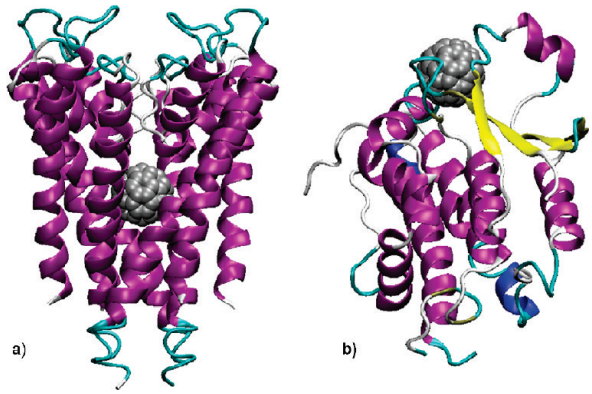

Figure 1. Fullerene docking for (a) voltage-gated potassium channel (PDB 1JVM) and (b) chlorine channel (PDB 2AHE).

cate that the inhibition occurs at the level of the chamber and not of the entry region as previously proposed.[11]

Ranks 2 and 3 are occupied by a glucocorticoid-like receptor and a glucocorticoid receptor. These receptors are not present in the set discussed in the previous section. They are presented here because of their importance and because the results of present analysis shows that many of the top 10% of the most binding proteins bind to steroid hormones and their derivatives. More in detail, the list of proteins that bind to steroid hormones and their derivatives includes pregnane X receptor, cholesterol esterase, Fab′ fragment of the Db3 anti-steroid monoclonal antibody, estrogen receptor α, estrogenic 17-β-hydroxysteroid dehydrogenase, retinoid X receptor, farnesoid X receptor, mammalian PCB-binding protein, liver X receptor β, 3-α-hydroxysteroid deydrogenase, estrogen receptor β, nuclear orphan receptor Lxr-β, and peroxisome proliferator activated receptor γ, which are ranked 9, 14, 17, 18, 23, 30, 32, 37, 40, 43, 62, 93, and 116.

It was previously proposed that the Fab′ fragment of mAb, which is specific for progesterone, can bind to C_{60}[20] because the chemical characteristics and dimensions of C_{60} and progesterone are very similar. Progesterone is 5.8 × 13 Å, while C_{60} is a sphere of 7.2 Å of diameter, which makes the surface area of the two molecules similar. The steroids binding site are hydrophobic cavities rich in Trp, Phe, and Tyr groups,[60] and the π-system of fullerene can interact with these residues. Experimentally, there is some evidence, even if not direct binding enzymatic assay, that C_{60}, during inhibition of allergic response, can affect significantly (more than 100-fold) protein signaling of progesterone receptor.[57]

Figure 2 shows the crystal structure of proteins that bind to steroids. The four structures are quite different from each other since a, b, and c are receptors, while d is an antibody. The docking procedure does not have any information about the binding area; the approach automatically searches the entire surface of a protein and finds the same crystallographic binding pockets identified for steroid hormones.

Rank 11 is occupied by acetylcholinesterase, AChE. Cholinesterases are a family of enzymes that contain a hydrophobic cavity that can accommodate a fullerene.[61] In AChE, the principal site,[62] where the cata-

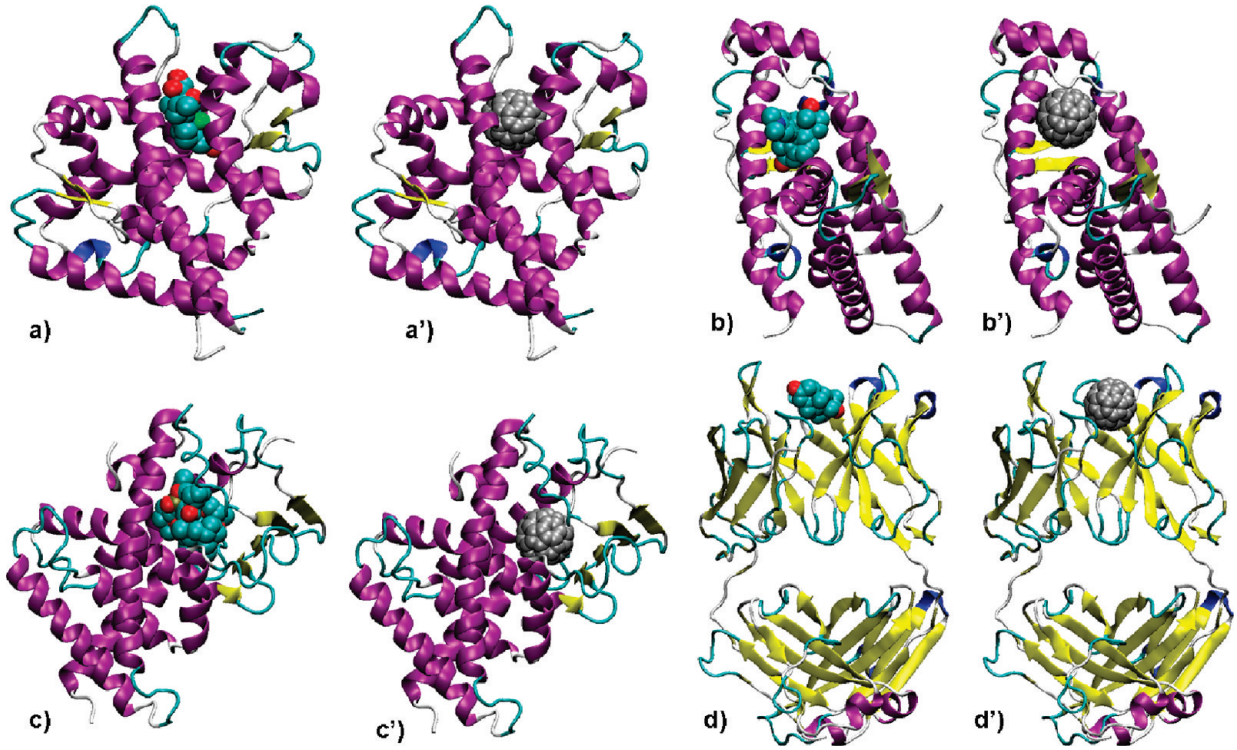

Figure 2. Crystallographic and docked structures of (a) 1NHZ, (b) 1P93, (c) 1ILH, and (d) 1DBB. The crystallographic structures contain the inhibitor; the docked structures, identified with a prime, contain C_{60}.

lytic triad is located, is at the bottom of a gorge ~20 Å deep. There is also a peripheral site, located near the edge of the cavity. The two sites are about 15 Å apart and are surrounded by the rings of 14 conserved aromatic residues.[63] The size of C_{60} suggested that it could be accommodated into the hydrophobic core of AChE. Fullerene derivatives were designed and the inhibitory activity was evaluated.[56] Our approach identifies automatically AChE as a fullerene binding protein.

Figure 3 explains why C_{60} is a noncompetitive, low-affinity inhibitor and differs from competitive and more efficient inhibitors such as edrophonium chloride or tacrine. These quaternary charged ligands bind the active site,[64] while the fullerene occupies the hydrophobic cavity of AChE, hindering access of a substrate.

Rank 21 is occupied by nitric oxide synthase, NOS,[53] that is known to be inactivated by C_{60} derivatives. Fullerene adducts do not resemble structurally any of the known substrates or cofactors of NOS and it is not clear *a priori* where the interaction site of fullerene is located.[53] The fullerene binding pocket is here identified in terms of residues inside a sphere of 5 Å from C_{60} that consists of Trp180, Arg185, Cys186, Val187, Gly188, Arg189, Val338, Phe355, Ser356, Gly357, Trp358, Tyr359, Met360, Glu363, and Trp449.

Figure 4 shows the tight fit of C_{60} inside the pocket. The composition of the binding site is typical for hydrophobic interactions: it is rich in aromatic residues able to give $\pi-\pi$ interactions with C_{60} and charged residues for cation$-\pi$ interactions.

Rank 29 is occupied by troponin C, which has given indirect evidence of possible C_{60}-binding activity.[13] It is commonly accepted that C_{60} can bind to Ca^{2+} binding domains, because calmodulin also binds C_{60}. However, parvalbumin, a protein with three high-affinity Ca^{2+} binding sites in the EF-hand domain, can not bind C_{60}.[13]

Figure 5 shows that fullerene binds between the two lobes of the protein. In the crystal structure, 1DTL,[65] this position is occupied by one of the calcium-sensitizers, namely, bepridil, and C_{60} does not bind the EF-hand domain.

Rank 31 is occupied by cytochrome P450, which is recognized as a fullerene binding protein.[51] The binding site of C_{60} located by the present procedure does not coincide with the active site, Figure 6.

Because of the high ranking, it can be suggested that C_{60} triggers a protein rearrangement and inhibits the activity by an allosteric change of either P450 enzyme itself or NADPH-cytochrome P450 reductase. This suggestion is in accordance with the experimental results showing that fullerenol did not exhibit a competitive type of inhibition with substrates such as benzo[a]pyrene, 7-ethoxycoumarin, and NADPH.[51] The absence of competitive inhibition seems to indicate that C_{60} may be too bulky to compete with these molecules for binding to the active site of the enzyme.

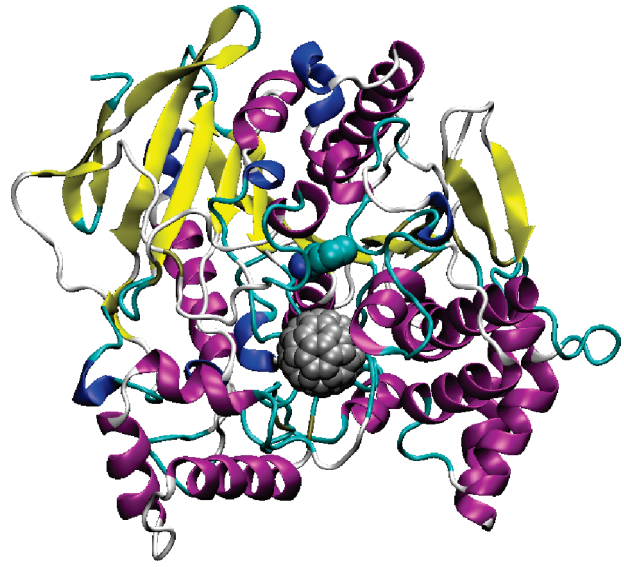

Figure 3. Docked structure of acetylcholinesterase. The crystallographic structure contained the tacrine inhibitor; the docked structure contains C_{60}.

Ranks 35 and 47 are occupied by Na,K-ATPase and bovine mithocondrial F1-ATPase, respectively. Na,K-ATPase hydrolyzes ATP to drive the coupled extrusion and uptake of Na^+ and K^+ ions across the plasma membrane. Bovine mitochondrial F1-ATPase is the prime producer of ATP, using the proton gradient generated by oxidative phosphorylation. Mitochondrial Mg^{2+}-ATPase activity is markedly inhibited by fulleronol with an IC_{50} values of 7.1 μM.[60]

Figure 7 shows that C_{60} does not bind in the ATP binding pocket. In both systems, its binding could be described as a ball blocking a gear. In Na,K-ATPase, C_{60} binds in the very mobile region delimited by Gln396-Ala416.[66] In F1-ATPase, C_{60} binds between the α and β subunits of the protein,[67] hindering the rotational movement necessary for the functioning of the protein.

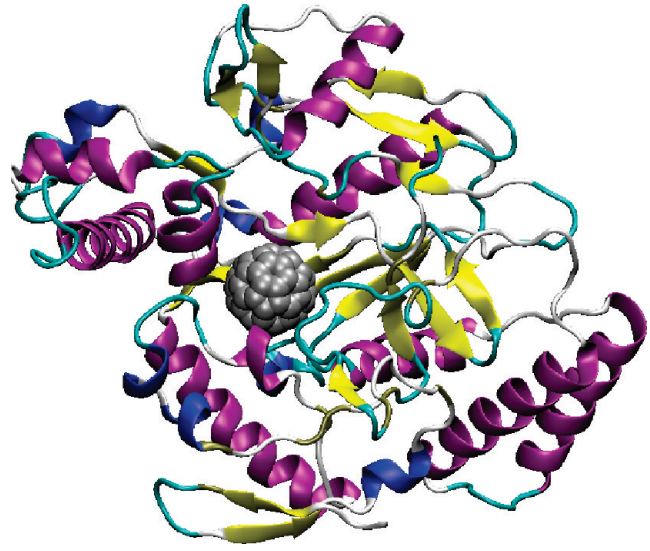

Figure 4. Docked complex of nitric oxide synthase, 2NSE, and C_{60}.

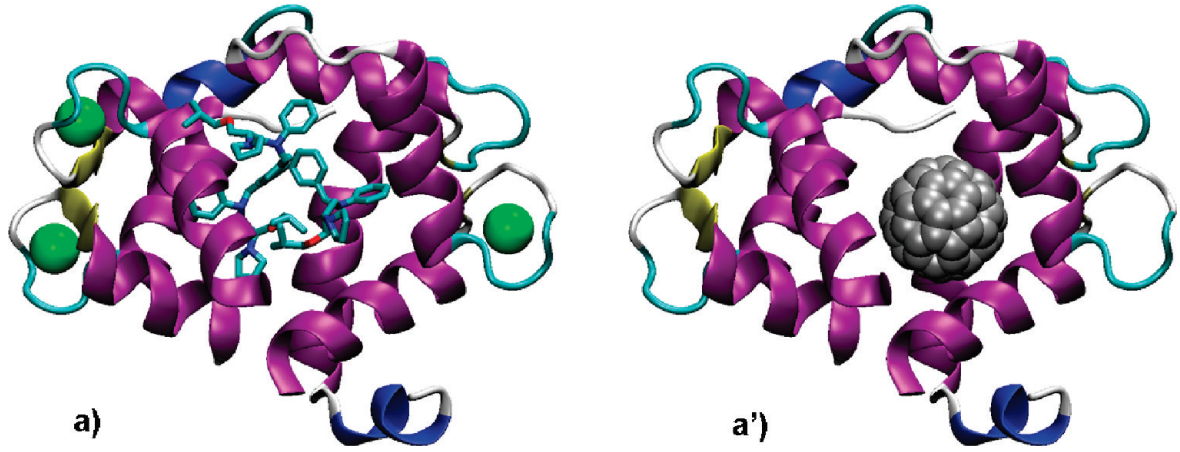

Figure 5. (a) Crystallographic structure of troponin C, 1DTL, with three calcium ions represented by green spheres and the bepridil molecule; (a′) Docked complex of troponin C and C_{60}.

Rank 42 is occupied by the microtubule protein. Fullerenol can inhibit tumor cell growth by blocking the microtubule assembly *in vitro*, which means that the rate and extension of microtubule formation can be influenced by C_{60} presence.[52] The binding pocket is located in the globular region of the protein that interacts with microtubules and with adenosine triphosphate (ATP) and that forms the motor domain,[68] see Figure 8.

Rank 46 is occupied by glutathione reductase. The inhibitory effects of C_{60} derivatives on glutathione reductase is known,[14] but the binding pocket remains unidentified. In the docked structure, Figure 9, the residues responsible for the binding are Ser 225, Phe226, Asp227, Ala336, Leu338, Tyr364, Asn366, Ile367, Pro368, Thr369, Thr379, Val380, Gly381, Leu382, and Thr383.

Rank 58 is occupied by cathepsin B (cysteine proteinases). This cysteine protease is known to bind

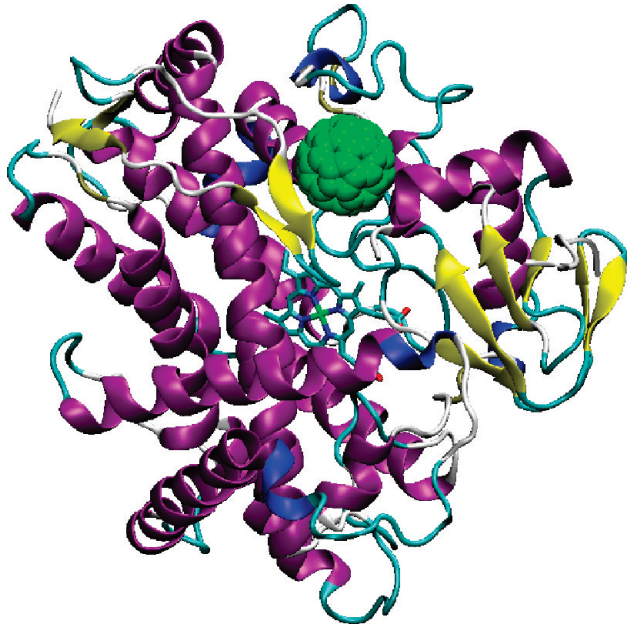

Figure 6. Docked complex of human cytochrome P450, 2F9Q, and C_{60}; the heme group is shown.

C_{60}[15,49] as thrombin and serine proteinase α-thrombin,[15,49] which are ranked 95 and 102. Figure 10 illustrates the binding pockets of this class of proteins. In cathepsin B and α-thrombin, C_{60} occupies the S1′ binding site.[69]

Rank 69 is occupied by HIV-reverse transcriptase. The anti-HIV activity of C_{60} is usually associated with HIV-protease inhibition. Recent studies demonstrated that also the activity of HIV-reverse transcriptase is affected by presence of fullerene.[55] The binding site, Figure 11, is in the P51 subunits, in the palm subdomain.[70,71]

Rank 74 is occupied by phosphoinositide 3-kinase. The activity of this kinase is affected by C_{60}.[57] The docked complex of Figure 12 shows that the binding site is close to the ATP binding pocket.

Rank 115 is occupied by glutathione S-transferase. Inhibition of this transferase by fullerene has been reported.[50] The docked structure, Figure 13, finds that the C_{60} binding pocket is in the same area of the glutathione binding pocket. The presence of C_{60} displaces the glutathione cofactor and inhibits functioning.

Rank 118 is occupied by HIV protease (Figure 14), probably the most known and characterized fullerene binding protein.[16−19] C_{60} binds to the cylindrically shaped pocket marked by residues Asp25, Asp25′, Ile50, and Ile50′. The only minor difference with what reported in the literature is that our refined optimization no longer makes the docking perfectly symmetric.[72]

Reverse docking procedures are considered successful if they identify 50% of the targets within the top 10%.[59] The present results are close to 80%. The four apparent failures out of 19 target proteins are human serum albumin, lysozyme, glutamate receptor, and anti-Buckminsterfullerene antibody Fab fragment.

For human serum albumin, the procedure identifies the same binding pocket described as site 2 by Gozin and co-workers.[72] They did not provide a comparison with other proteins. For lysozime, the experimental binding is with fullerenol, while it is with pristine C_{60} in

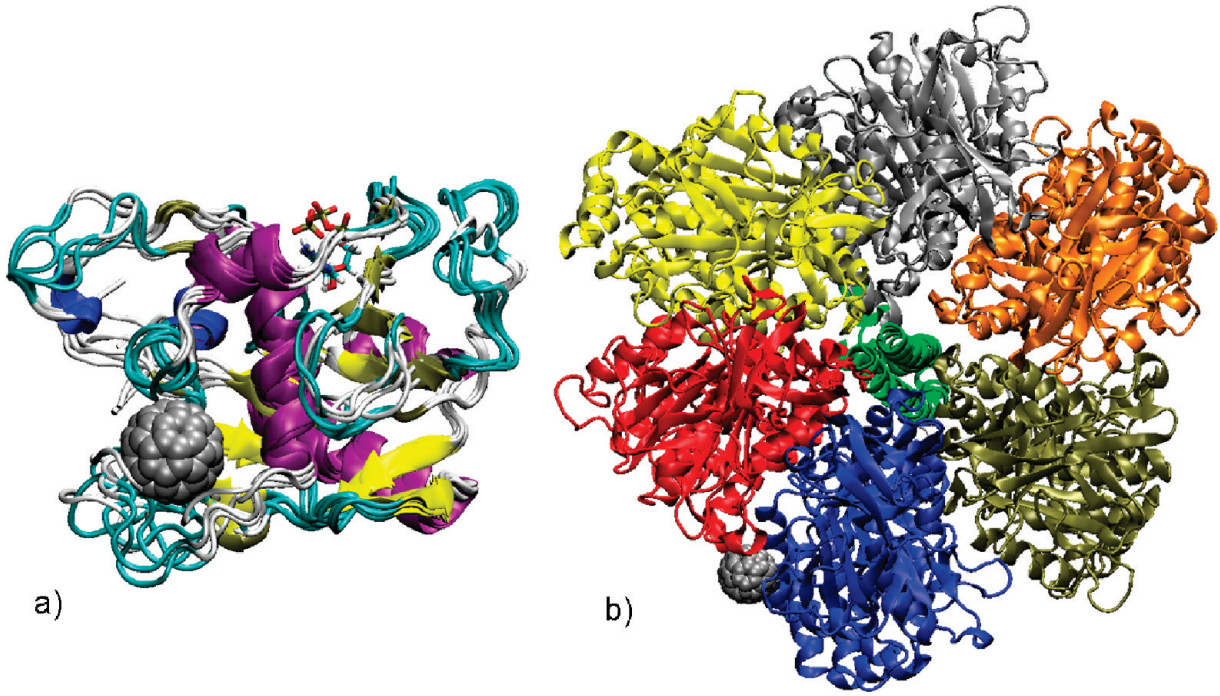

Figure 7. (a) Docked complex of binding domain of rat alpha1 Na,K-ATPase, 1MO8, and C_{60}. Only 4 NMR conformations of the 20 available are displayed for clarity. It is evident the mobility of the region in the fullerene binding pocket. ATP is represented. (b) Docked complex of mitochondrial F1-ATPase, 1EFR, and C_{60}. Different subunits are in different colors.

this work. The identified fullerenol binding site is characterized by two arginines that can form hydrogen bonds with oxidrils. Binding between C_{60} and anti-Buckminsterfullerene antibody Fab fragment involves an induced fit mechanism that is not present in our approach. Glutamate receptor are some of the most complex structures existing and no structure has been refined for the entire receptor. The X-ray structures existing for the various components of the quaternary assembly do not lend themselves to use in the docking for these proteins. The 15 out of 19 can be considered a lower limit and implies the good accuracy of the model used to assess C_{60}—protein binding and its ability to account for the interactions in these hybrid systems.

Predictive Power: Searching for Further Evidence. The accuracy of the model warrants a closer exam of the top scorers. The intent is not only to provide more details, but also to suggest possible future uses of C_{60}.

In Table 1, rank 1 is occupied by a potassium channel, which has been discussed in detail in the previous section.

Steroid hormone receptors[73] occupy 4 out of the first 10 positions in the table. The interaction of C_{60} and steroid hormone receptors, SHR, is a well-recognized pattern. SHRs represent one of the pharmaceutically important families of drug targets[73] because these receptors are generally expressed in a broad range of tissues and play roles in multiple physiological pathways. More specifically, positions 2 and 3 are occupied by glucocorticoid-like and glucocorticoid receptors. Glucocorticoid agonists are the most effective anti-inflammatory drugs available for a wide spectrum of conditions including asthma and rheumatoid arthritis.[74,75] The possible interest for the development of a completely new class of inhibitors based on fullerene derivatives could be high.[76]

Inosine 5′-monophosphate dehydrogenase, IMPDH, is ranked 4. IMPDH has emerged as an attractive therapeutic target for the treatment of various conditions[77] including cancer[78] and viral infections.[79] IMPDH inhibitors have also been used clinically as immunosuppressants, prompting further interest in utilizing this class of therapeutics for treating other autoimmune diseases.[80] IMPDH strong interaction with C_{60} may lead to the development of new inhibitors.

Glycinamide ribonucleotide formyltransferase, GARFT, is ranked 5. GARFT is an attractive target site

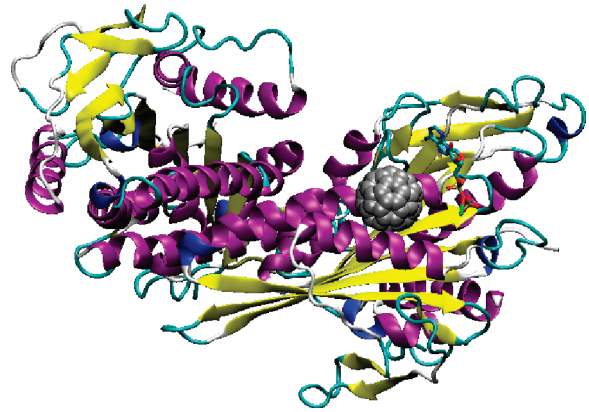

Figure 8. Docked complex of microtubule motor protein, ncd 1CZ7, and C_{60}.

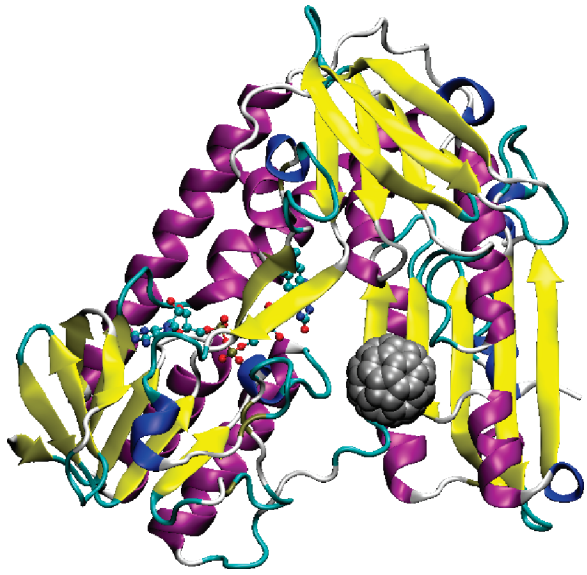

Figure 9. Docked complex of glutathione reductase, 1XAN, and C_{60}.

for anticancer chemotherapy. Its inhibition hinders the *de novo* purine biosynthesis that is in high demand by proliferative tumor cells. As in the case of GARFT, C_{60} may also inhibit other enzymes involved in the folate metabolism as dihydrofolate reductase (ranked 8) or thymidylate synthase (ranked 25). Inhibitors of these two proteins found clinical utility as antitumor, antimicrobial, and antiprotozoal agents.[81−84]

Lumazine synthase, LS, is ranked 6. Lumazine synthase is involved in the last steps of the biosynthesis of riboflavin, vitamin B_2. Riboflavin plays a crucial role in many biological processes, including photosynthesis and mitochondrial electron transport. While animals obtain riboflavin from dietary sources, numerous microorganisms, including Gram-negative pathogenic bacteria and yeasts, lack an efficient riboflavin uptake system and therefore depend on endogenous riboflavin biosynthesis.[85] Riboflavin biosynthesis offers attractive targets for the design and synthesis of new antibiotics.

2,4-Dienoyl-CoA reductase is ranked 7. 2,4-Dienoyl-CoA reductase is involved in the metabolism of all unsaturated fatty acids with double bonds starting at even-numbered positions, and some unsaturated fatty acids with double bonds starting at odd-numbered positions, regardless of the stereochemical configuration of the double bonds.[886] Numerous diseases have been reported in relation to fatty acids, such as cardiovascular disease,[87] cancer,[88] and diabetes.[89] Inhibitors of en-

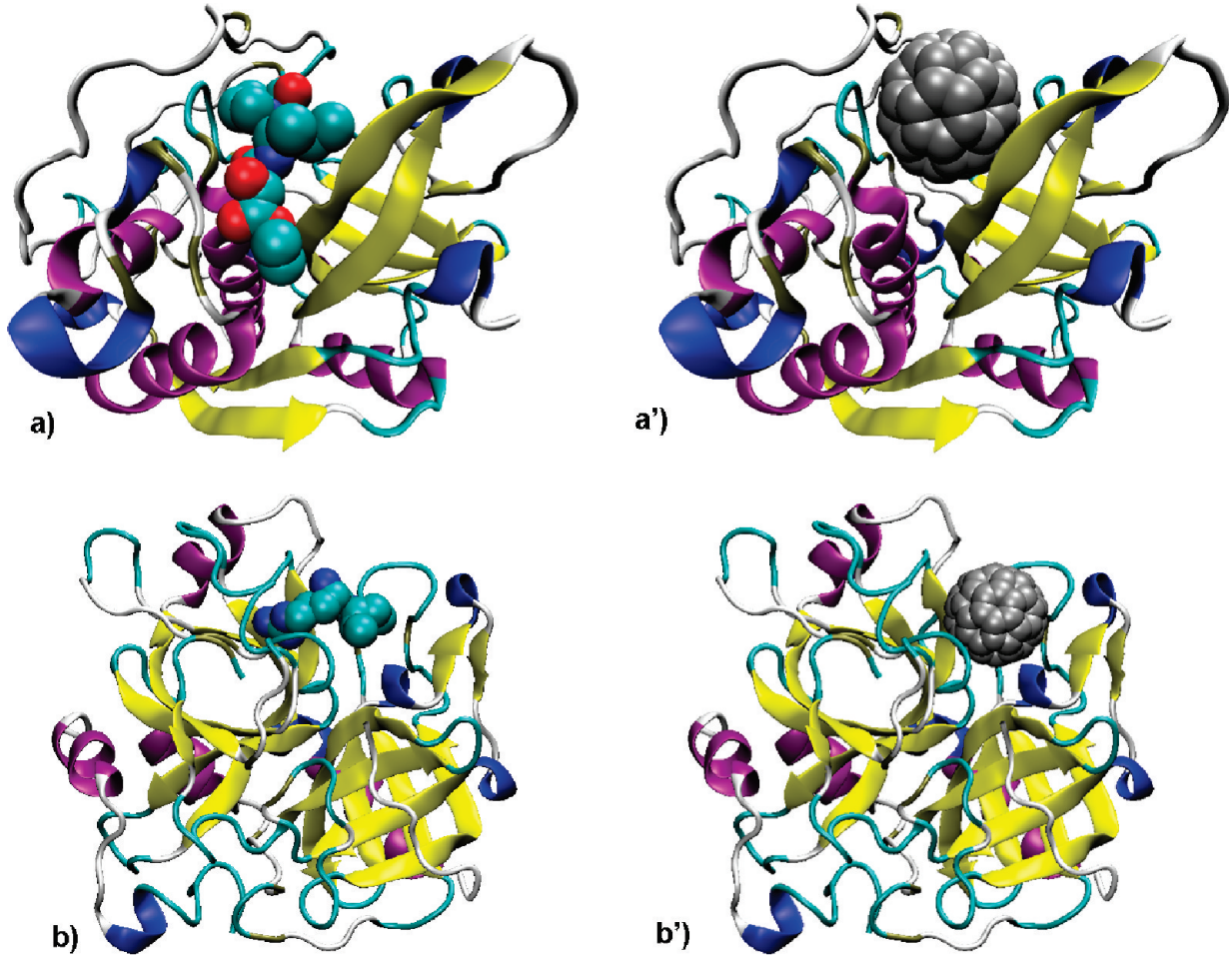

Figure 10. (a) Complex of cathepsin B, 1CSB, and crystallographic inhibitor CA030; (a′) Docked structure C_{60} cathepsin B and C_{60}; (b) Complex of α-thrombin, 1A4W, and RWJ-50353, RWJ-50215 inhibitors; (b′) Docked complex of α-thrombin and C_{60}.

zymes involved in the metabolism of fatty acids have been synthesized and studied as potential medicines a to treat noninsulin dependent diabetes mellitus (NIDDM).[90]

Dihydrofolate reductase, DHFR, is ranked 8. It is interesting to discuss this enzyme in conjunction with serine hydroxymethyltransferase, SHMT, rank 24, and thymidylate synthase, TS, rank 25. Most eukaryotic organisms synthesize the essential metabolite thymidylate *via* the thymidylate cycle, which consists of these three enzymes. Inhibition of TS or of DHFR leads to "thymineless death" in the absence of salvage,[91] and inhibition of these enzymes has found clinical use as antitumor, antimicrobial, and antiprotozoal agents.[92,93] C_{60} inhibits all three enzymes. Design of a single agent that functions as multiple inhibitors against TS and DHFR could be very important.[94−97] Such inhibitor could circumvent pharmacokinetic, drug−drug interactions, and toxicity disadvantages of administering two separate agents in combination chemotherapy protocols. C_{60} derivatives appear to be a possible target for a trivalent inhibitor. These systems could also overcome a disadvantage of classical antifolates antitumor agents that require an active transport mechanism[98] to enter cells, which, when impaired, causes tumor resistance.[99,100] The ability of C_{60} to be passively transported into the cell could be a further benefit in the development of a drug.[101]

Pregnane X receptor, PXR, is ranked 9. PXR is the primary xenobiotic sensor in human and mammalian tissues.[102] It responds to a wide range of structurally and chemically distinct ligands that range from small lipophilic drugs to potentially toxic bile acids as well as cholesterol metabolites. In addition to its main function in the detoxification of xeno- and endobiotic toxicants, PXR has also been implicated in many endobiotic functions, ranging from cholestatic prevention[103,104] to bilirubin detoxification and clearance, adrenal steroid homeostasis, drug−hormone interactions,[105] lipid metabolism,[106] inflammatory bowel disease,[107,108] bone homeostasis,[109] and retinoid acid metabolism.[110] There is increasing evidence that PXR activation leads to increased cancer cell growth and drug resistance.[111] In the context of cancer therapeutics, controlling PXR activation could provide therapeutic benefits by improving both drug metabolism and delivery, also because only a few PXR inhibitors have been described.[112−115]

Aldo-Keto reductase, A-KR, family 1 member C3 is ranked 10. This enzyme catalyzes the conversion of aldehydes and ketones to alcohols. It also converts active androgens, estrogens, and progestins and their cognate inactive metabolites[116] and preferentially transforms androstenedione (4-dione) to testosterone. It plays an important role in the pathogenesis of allergic diseases, such as asthma, and may also have a role in controlling cell growth and differentiation. Novel methods of treating and/or inhibiting development of prostatic cancer, benign prostatic hyperplasia, prostatitis, acne, seborrhea, hirsutism, or androgenic alopecia utilize inhibitors of 3-α-hydroxysteroid dehydrogenase alone or in combination with other active pharmaceuticals such as inhibitors of 17-β-hydroxysteroid dehydrogenase, HD. This enzyme is included in our list in position 23. C_{60} can represent a new class of inhibitors for both A-KR and HD.

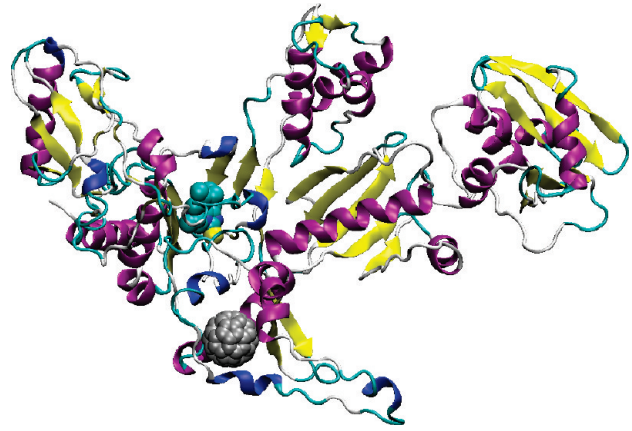

Figure 11. Docked complex of HIV-RT (1TVR) and C_{60}. The TIBO inhibitor, present in the crystallographic structure, is in VdW representation.

From the analysis of the top 10% list of fullerene binding proteins, other targets appear. For example, C_{60} seems to inhibit trypanothione reductase, rank 38. This enzyme is found in parasitic protozoal parasites such as leishmaniasis, sleeping sickness and Chagas' disease.[117] Because the enzyme is absent in humans and is essential for the survival of these parasites, it is a target for the development of new drugs. Also inhibition of ornithine decarboxylase, rank 52, can be an attractive target for fullerene inhibition, because it is an enzyme indispensable for parasites such as trypanosoma, giardia, and plasmodium. Other targets, economically rel-

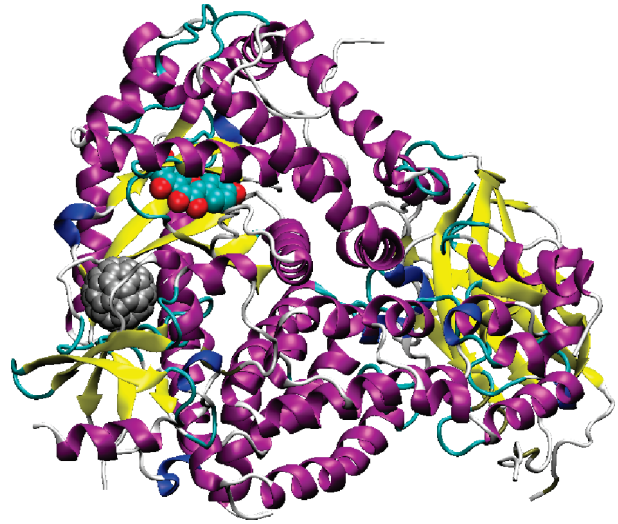

Figure 12. Docked complex of phosphoinositide 3-kinase, 1E8W, and C_{60}. The quercitin inhibitor, present in the crystallographic structure, is in VdW representation.

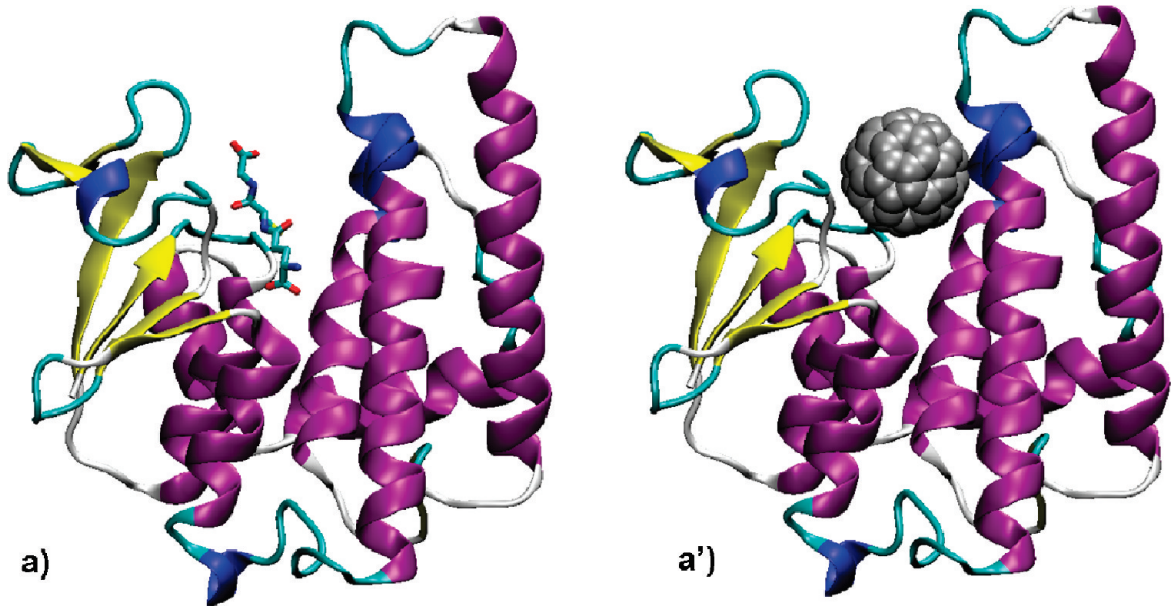

Figure 13. (a) Crystallographic structure of glutathione S-transferase, 1PMT, with glutathione shown; (a′) Docked complex of glutathione S-transferase and C_{60}.

evant, that can interact with fullerene are poliovirus type 1, mahoney strain, rank 57, or rhinovirus 14, HRV14, rank 85.

It is interesting that in the top 10% there are some antibodies that seem able to recognize C_{60}. They are immunoglobulin lambda light chain dimer, Mcg, rank 16, Fab′ fragment of the Db3 anti-steroid monoclonal antibody, rank 17, MGDF receptor, rank 44, MHC class I H-2KB heavy chain, rank 53, murine BR96 Fab, rank 70, murine MHC class I H-2Kb, rank 81, HIV-1 gp120 protein, rank 87, histocompatibility leukocyte antigen, Hla-Cw4 heavy chain, rank 92, Fab, rank 97, and immunoglobulin McPC603 Fab-phosphocoline, rank 99.

Table 1 can be an important source for the search of C_{60} binding proteins. As with all predictions, apart from the 4 out of 19 false negatives, a word of caution to the reader is that some false positive intruders may be present.

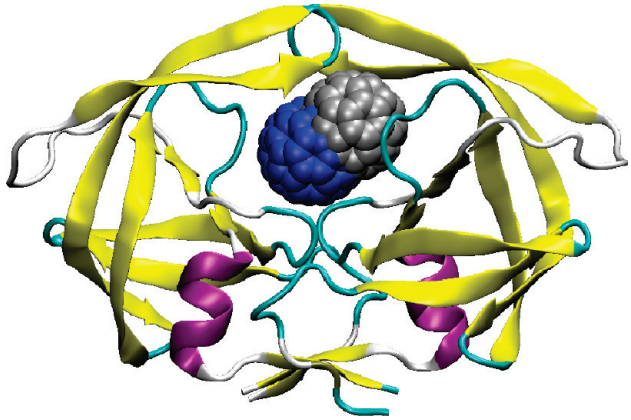

Figure 14. Predicted binding site of C_{60} with on HIV protease (1AID) by PatchDock[72] (blue sphere) and PatchDock followed by refinement with FireDock (silver sphere).

CONCLUSION

The experiments detailing the binding of C_{60} to HIV protease, cysteine and serine proteinases, glutathione S-transferase and reductase, cytochrome P450, ATPase, tubulin, antibody Fab fragment, glutamate receptors, nitric oxide synthase, troponin, ion channels, serum albumin, HIV-reverse transcriptase, acethylcholineaterase, lysozyme, and a set of proteins that inhibit allergic response provide clear evidence that C_{60} and proteins are a good if not perfect match.

A set of more than 1200 protein structures, which comprehend the proteins mentioned above, is examined by an algorithm that appraises quantitatively the interaction between C_{60} and the surface of each protein. The redundancy of the set of structures allows quantitative verification of the predictive power of the approach that find explicitly the most probable site where C_{60} docks for each protein.

The proteins are ranked for their binding to C_{60}. Position 1 is for voltage-gated potassium channel, 11 for acetylcholinesterase, 21 for nitric oxide synthase, 29 for troponin C, 31 for cytochrome P450, 35, and 47 for Na,K-ATPase and bovine mitochondrial F1-ATPase, 42 for the microtubule protein, 46 for glutathione reductase, 58 for cathepsin B (cysteine proteinases), 69 for HIV reverse transcriptase, 74 for phosphoinositide 3-kinase, 95 for thrombin, 102 for α-thrombin, 115 for gluthatione S-transferase, and 118 for HIV protease. The close match between the model and experiments vouches for the accuracy of the model and warrants for a closer exam of the top scorers, which are discussed also in view of possible future applications of C_{60}. The analysis of the 10 most binding proteins suggests a wide variety of pos-

sible applications that include (i) anti-inflammatory drugs, (ii) autoimmune diseases, (iii) antitumor, antimicrobial, and antiprotozoal therapies, (iv) new antibiotics, and (v) treatment of non-insulin-dependent diabetes mellitus.

Practical applications of fullerenes as biological, or pharmacological agents, require dosage and serum levels capable of measurement, preferably by sensitive and simple immunological procedures. This, in turn, requires that specific antibodies able to recognize fullerene should be produced. Many antibodies are present in Table 1 and strongly bind to C_{60}.

The comprehension of the interactions in protein-C_{60} hybrids by a simple model can also lead to the design and development of proteins or peptides that can carry C_{60} to a predetermined position for their supramolecular organization. Indeed, many of the enzymes listed in the top scorer Table 1 have been used as biosensors, in integrated biodevices, based on carbon nanotubes. Considering only the first 50 positions of the table, immobilized acetylcholinesterase, rank 11, is used as a biosensor for organophosphate pesticides and nerve agents,[118] cholesterol esterase,[119] rank 14, or cytochrome P450,[120] rank 31, for monitoring total cholesterol in blood, estrogen receptor α,[121] rank 18, to detect xenoestrogens that are at the basis of the increase of diseases related to the estrous cycle, among which, masculine infertility or increase in some types of cancers, oxidases,[122] rank 45, to sense glucose level and alcohol dehydrogenase,[123] rank 50, to quantify ethanol presence. It is well documented the use of C_{60} in bioelectrochemical sensors and all the proteins that can interact with C_{60} can be potentially be used in nanobiointegrated devices.[124]

METHODS

Proteins were screened for their potential binding to C_{60}. A feature of C_{60} crucial for this work is that the most important energy term that describes fullerene binding to proteins is the van der Waals interactions between the cage and the protein surface. Some fullerene derivatives may possess higher affinities than pristine C_{60} if the functionalizing groups form H-bonds with the residues of the protein. However, derivatization of C_{60} is often used only to increase its solubility in water, with the result that in the binding process the functional group remains exposed in the solvent. Exploration of issues related to C_{60} functionalization is beyond the purpose of this work, which is aimed at investigating the role of surface complementarity in the binding.

The database selected was the drug target database (PDTD).[47] PDTD is a comprehensive, web-accessible database of drug targets and focuses on those drug targets with known 3D structures. PDTD contains 1207 entries covering 841 known and potential drug targets with structures from the protein data bank (PDB). The coordinates of the proteins were isolated from the PDB. Because not all PDB structures are of equal quality, when it has several redundant records in PDB, a protein structure is selected according to the following criteria: (i) select the structure without mutation and missing residues around the active site; (ii) select the structure with high resolution; and (iii) select the structure complexed with ligand.[47] For each selected drug target of PDTD was categorized into 15 and 13 types according to two criteria: therapeutic areas and biochemical criteria. To take into account protein flexibility, PDTD includes redundant entries for proteins known to be flexible. Docking models were obtained using the PatchDock algorithm.[125] PatchDock takes as input two molecules and computes three-dimensional transformations of one of the molecules with respect to the other with the aim of maximizing surface shape complementarity, while minimizing the number of steric clashes. Given a protein and a molecule, PatchDock first divides their surfaces into patches according to the surface shape (concave, convex, or flat). Then, it applies the geometric hashing algorithm to match concave patches with convex patches and flat patches with flat patches and generates a set of candidate transformations. Each candidate transformation is further evaluated by a set of scoring functions that estimate both the shape complementarity and the atomic desolvation energy[126] of the complex. These terms are the most important in the case of binding of fullerene with proteins and the algorithm has been demonstrated to work perfectly to recognize these interactions.[72] Redundant solutions are discarded by use of rmsd (root-mean-square deviation) clustering. PatchDock is highly efficient, because it utilizes advanced data structures and spatial pattern detection techniques, which are based on matching of local patches. The local shape information is then extended and integrated to achieve global solutions. The algorithm implicitly addresses surface flexibility by allowing minor penetrations. Accurate rescoring of the complexes is then carried out using FireDock program.[127] This method simultaneously targets the problem of flexibility and scoring of solutions produced by fast rigid-body docking algorithms.

Possible readjustments of the protein structure in the presence of the solvent are accounted for. Redundant entries are present in the database for proteins known to be flexible, side-chain flexibility is modeled by rotamers and Monte Carlo minimization.[128] Following the rearrangement of the side-chains, the relative position of the docking partners is refined by Monte Carlo minimization of the binding score function.

Desolvation free energy in the binding process is taken into account by a solvation model using estimated effective atomic contact energies (ACE).[126]

All the candidates are ranked by a binding score.[127] This score includes, in addition to atomic contact energy,[126] van der Waals interactions, partial electrostatics, explicit hydrogen and disulfide bonds contribution, π-stacking, and cation$-\pi$ interaction. The electrostatic contribution for protein$-$fullerene binding energy is zero because all charges of carbon atoms on fullerene are zero as well as explicit hydrogen and disulfide bonds contribution. The most important contribution derives from van der Waals energy (E_{VdW}). E_{VdW} between two atoms a_i and a_j is defined as the modified Lennard-Jones 6$-$12 potential with linear short-range repulsive score,[127,129] i.e.,

$$E_{VdW(a_i,a_j)} = \begin{cases} \varepsilon_{ij}\left(\dfrac{\sigma_{ij}^{12}}{r_{ij}^{12}}\right) - 2\dfrac{\sigma_{ij}^{6}}{r_{ij}^{6}} & , \quad r_{ij} > 0.6\sigma_{ij} \\ \varepsilon_{ij}(A + B(r_{ij} - 0.6\sigma_{ij})), & \text{otherwise} \end{cases} \tag{1}$$

where

$$A = \frac{\sigma_{ij}^{12}}{(0.6\sigma_{ij})^{12}} - 2\frac{\sigma_{ij}^{6}}{(0.6\sigma_{ij})^{6}}, \quad B = -12\frac{\sigma_{ij}^{12}}{(0.6\sigma_{ij})^{13}} + 12\frac{\sigma_{ij}^{6}}{(0.6\sigma_{ij})^{7}} \tag{2}$$

The parameter σ_{ij} is the atomic radii sum and the parameter ε_{ij} is the energy well depth, derived from the CHARMM19 force field.[130] The hydrogen atomic radii are reduced by 40% because of their uncertain positions. All the energy terms are calculated inside a 6 Å radius of interatomic distance.

Three additional components to the total binding score are added: $E_{pi\text{-}pi}$ for the $\pi-\pi$ interactions, $E_{cat\text{-}pi}$ for the cation$-\pi$ interactions and E_{aliph} for the aliphatic interactions. These are the

interactions of the positive amines of Lys or Arg with the π-electron cloud of the aromatic side chains (Phe, Tyr, Trp), π−π interactions occur between the aromatic residues Phe, Tyr, His, Trp, and Pro, and the aliphatic pairs consist of Leu, Ile, and Val. These values are parametrized following the work of Misura *et al.*[131]

The scoring function used here has been extensively and successfully tested on protein−protein docking benchmark of ~80 complexes and on all the CAPRI targets.[132]

Acknowledgment. We would like to thank Daniele Ciabattoni for assistance with the graphics.

Supporting Information Available: Extended version of Table 1 with related disease and scoring function columns. This material is available free of charge *via* the Internet at http://pubs.acs.org.

REFERENCES AND NOTES

1. Karajanagi, S. S.; Asuri, P.; Sellitto, E.; Eker, B.; Bale, S. S.; Kane, R. S.; Dordick, J. S. *Protein−Carbon Nanotube Conjugates*; ACS Symposium Series 986, American Chemical Society: Washington, DC, 2008; pp 1020−1115.
2. Bosi, S.; Da Ros, T.; Spalluto, G.; Prato, M. Fullerene Derivatives: an Attractive Tool for Biological Application. *Eur. J. Med. Chem.* **2003**, *38*, 913–923.
3. Prato, M. Fullerene Chemistry for Materials Science Applications. *J. Mater. Chem.* **1997**, *7*, 1097–1109.
4. Nel, A.; Xia, T.; Madler, L.; Li, N. Toxic Potential of Materials at the Nanolevel. *Science* **2006**, *311*, 622–627.
5. Maynard, A. D.; Aitken, R. J.; Butz, T.; Colvin, V.; Donaldson, K.; Oberdorster, G.; Philbert, M. A.; Ryan, J.; Seaton, A.; Stone, V.; et al. Safe Handling of Nanotechnology. *Nature* **2006**, *444*, 267–269.
6. Da Ros, T.; Prato, M.; Novello, F.; Maggini, M.; Banfi, E. Easy Access to Water-Soluble Fullerene Derivatives *via* 1,3-Dipolar Cycloadditions of Azomethine Ylides to C_{60}. *J. Org. Chem.* **1996**, *61*, 9070–9072.
7. Dugan, L. L.; Turetsky, D. M.; Du, C.; Lobner, D.; Wheeler, M.; Almli, C. R.; Shen, C. K.; Luh, T. Y.; Choi, D. W.; Lin, T. S. Carboxyfullerenes as Neuroprotective Agents. *Proc. Natl. Acad. Sci. U.S.A.* **1997**, *94*, 9434–9439.
8. Jin, H.; Chen, W. Q.; Tang, X. W.; Chiang, L. Y.; Yang, C. Y.; Schloss, J. V.; Wu, J. Y. Polyhydroxylated C_{60}, Fullerenols, as Glutamate Receptor Antagonists and Neuroprotective Agents. *J. Neurosci. Res.* **2000**, *62*, 600–607.
9. Boutorine, A. S.; Tokuyama, H.; Takasugi, M.; Isobe, H.; Nakamura, E.; Helene, C. Fullerene-Oligonucleotide Conjugates: Photoinduced Sequence-Specific DNA Cleavage. *Angew. Chem., Int. Ed.* **1994**, *33*, 2426–2465.
10. Huang, Y. L.; Shen, C. K.; Luh, T. Y.; Yang, H. C.; Hwang, K. C.; Chou, C. K. Blockage of Apoptotic Signaling of Transforming Growth Factor-β in Human Hepatoma Cells by Carboxyfullerene. *Eur. J. Biochem.* **1998**, *254*, 38–43.
11. Park, K. H.; Chhowalla, M.; Iqbal, Z.; Sesti, F. Single-Walled Carbon Nanotubes Are a New Class of Ion Channel Blockers. *J. Biol. Chem.* **2003**, *278*, 50212–50216.
12. Kim, J. E.; Lee, M. Fullerene Inhibits β-Amyloid Peptide Aggregation. *Biochem. Biophys. Res. Commun.* **2003**, *303*, 576–579.
13. Wolff, D. J.; Barbieri, C. M.; Richardson, C. F.; Schuster, D. I.; Wilson, S. R. Trisamine C_{60}-Fullerene Adducts Inhibit Neuronal Nitric Oxide Synthase by Acting as Highly Potent Calmodulin Antagonists. *Arch. Biochem. Biophys.* **2002**, *399*, 130–141.
14. Mashino, T.; Okuda, K.; Hirota, T.; Hirobe, M.; Nagano, T.; Mochizuki, M. Inhibitory Effect of Fullerene Derivatives on Glutathione Reductase. *Fullerene Sci. Technol.* **2001**, *9*, 191–196.
15. Tokuyama, H.; Yamago, S.; Nakamura, E.; Shiraki, T.; Sugiura, Y. Photoinduced Biochemical Activity of Fullerene Carboxylic Acid. *J. Am. Chem. Soc.* **1993**, *115*, 7918–7919.
16. Friedman, S. H.; DeCamp, D. L.; Sijbesma, R.; Srdanov, G.; Wudl, F.; Kenyon, G. L. Inhibition of the HIV-1 Protease by Fullerene Derivatives: Model Building Studies and Experimental Verification. *J. Am. Chem. Soc.* **1993**, *115*, 6506–6509.
17. Marcorin, G. L.; Da Ros, T.; Castellano, S.; Stefancich, G.; Bonin, I.; Miertus, S.; Prato, M. Design and Synthesis of Novel [60]Fullerene Derivatives as Potential HIV Aspartic Protease Inhibitors. *Org. Lett.* **2000**, *2*, 3955–3958.
18. Schuster, D. I.; Wilson, S. R.; Schinazi, R. F. Anti-Human Immunodeficiency Virus Activity and Cytotoxicity of Derivatized Buckminsterfullerenes. *Bioorg. Med. Chem. Lett.* **1996**, *6*, 1253–1256.
19. Sijbesma, R.; Srdanov, G.; Wudl, F.; Castoro, J. A.; Friedman, S. H.; DeCamp, D. L.; Kenyon, G. L. Synthesis of a Fullerene Derivative for the Inhibition of HIV Enzymes. *J. Am. Chem. Soc.* **1993**, *115*, 6510–6512.
20. Chen, B. X.; Wilson, S. R.; Das, M.; Coughlin, D. J.; Erlanger, B. F. Antigenicity of Fullerenes: Antibodies Specific for Fullerenes and Their Characteristics. *Proc. Natl. Acad. Sci. U.S.A.* **1998**, *95*, 10809–10813.
21. Braden, B. C.; Goldbaum, F. A.; Chen, B. X.; Kirschner, A. N.; Wilson, S. R.; Erlanger, B. F. X-Ray Crystal Structure of an Anti-Buckminsterfullerene Antibody Fab Fragment: Biomolecular Recognition of C_{60}. *Proc. Natl. Acad. Sci. U.S.A.* **2000**, *97*, 12193–12197.
22. Belgorodsky, B.; Fadeev, L.; Ittah, V.; Benyamini, H.; Zelner, S.; Huppert, D.; Kotlyar, A. B.; Gozin, M. Formation and Characterization of Stable Human Serum Albumin-Tris-Malonic Acid [C_{60}]Fullerene Complex. *Bioconjugate Chem.* **2005**, *16*, 1058–1062.
23. Rozhkov, S. P.; Goryunov, A. S.; Sukhanova, G. A.; Borisova, A. G.; Rozhkova, N. N.; Andrievsky, G. V. Protein Interaction with Hydrated C_{60} Fullerene in Aqueous Solutions. *Biochem. Biophys. Res. Commun.* **2003**, *303*, 562–566.
24. Bingshe, X.; Xuguang, L.; Xiaoqin, Y.; Jinli, Q.; Weijun, J. Studies on the Interaction of Water-Soluble Fullerols with BSA and Effects of Metallic Ions. *Mater. Res. Soc. Symp.* **2001**, W7.4.1W7.4.5.
25. Yang, S.-T.; Wang, H.; Guo, L.; Gao, Y.; Liu, Y.; Cao, A. Interaction of Fullerenol with Lysozyme Investigated by Experimental and Computational Approaches. *Nanotechnology* **2008**, *19*, 395101.
26. Zheng, M.; Jagota, A.; Semke, E. D.; Diner, B. A.; McLean, R. S.; Lustig, S. R.; Richardson, R. E.; Tassi, N. G. DNA-Assisted Dispersion and Separation of Carbon Nanotubes. *Nat. Mater.* **2003**, *2*, 338–342.
27. Kam, N. W. S.; Liu, Z. A.; Dai, H. J. Carbon Nanotubes as Intracellular Transporters for Proteins and DNA: An Investigation of the Uptake Mechanism and Pathway. *Angew. Chem., Int. Ed.* **2006**, *45*, 577–581.
28. Tromp, R. M.; Afzali, A.; Freitag, M.; Mitzi, D. B.; Chen, Z. Novel Strategy for Diameter-Selective Separation and Functionalization of Single-Wall Carbon Nanotubes. *Nano Lett.* **2008**, *8*, 469–472.
29. Nepal, D.; Balasubramanian, S.; Simonian, A. L.; Davis, V. A. Strong Antimicrobial Coatings: Single-Walled Carbon Nanotubes Armored with Biopolymers. *Nano Lett.* **2008**, *8*, 1896–1901.
30. Feldman, A. K.; Steigerwald, M. L.; Guo, X.; Nuckolls, C. Molecular Electronic Devices Based on Single-Walled Carbon Nanotube Electrodes. *Acc. Chem. Res.* **2008**, *41*, 1731–1741.
31. Staii, C.; Johnson, A. T.; Chen, M.; Gelperin, A. DNA-Decorated Carbon Nanotubes for Chemical Sensing. *Nano Lett.* **2005**, *5*, 1774–1778.
32. Chen, R. J.; Bangsaruntip, S.; Drouvalakis, K. A.; Wong Shi Kam, N.; Shim, M.; Li, Y.; Kim, W.; Utz, P. J.; Dai, H. Noncovalent Functionalization of Carbon Nanotubes for Highly Specific Electronic Biosensors. *Proc. Natl. Acad. Sci. U.S.A.* **2003**, *100*, 4984–4989.
33. Sarikaya, M.; Tamerler, C.; Jen, A. K.-Y.; Schulten, K.; Baneyx, F. Molecular Biomimetics: Nanotechnology Through Biology. *Nat. Mater.* **2003**, *2*, 577–585.
34. Nednoor, P.; Capaccio, M.; Gavalas, V. G.; Meier, M. S.; Anthony, J. E.; Bachas, L. G. Hybrid Nanoparticles Based on Organized Protein Immobilization on Fullerenes. *Bioconjugate Chem.* **2004**, *15*, 12–15.

35. Tamerler, C.; Sarikaya, M. Genetically Designed Peptide-Based Molecular Materials. *ACS Nano* **2009**, *3*, 1606–1614.
36. Harding, J. H.; Duffy, D. M.; Sushko, M. L.; Rodger, P. M.; Quigley, D.; Elliott., J. A. Computational Techniques at the Organic−Inorganic Interface in Biomineralization. *Chem. Rev.* **2008**, *108*, 4823–4854.
37. Oren, E. E.; Tamerler, C.; Sahin, D.; Hnilova, M.; Seker, U. O. S.; Sarikaya, M.; Samudrala, R. A Novel Knowledge-Based Approach for Designing Inorganic Binding Peptides. *Bioinformatics* **2007**, *23*, 2816–2822.
38. Shoichet, B. K. Virtual Screening of Chemical Libraries. *Nature* **2004**, *432*, 862–865.
39. Kitchen, D. B.; Decornez, H.; Furr, J. R.; Bajorath, J. Docking and Scoring in Virtual Screening for Drug Discovery: Methods and Applications. *Nat. Rev. Drug Discovery* **2004**, *3*, 935–949.
40. Klebe, G. Virtual Ligand Screening: Strategies, Perspectives and Limitations. *Drug Discovery Today* **2006**, *11*, 580–594.
41. Jorgensen, W. L. Efficient Drug Lead Discovery and Optimization. *Acc. Chem. Res.* **2009**, *42*, 724–733.
42. Durdagi, S.; Supuran, C. T.; Strom, T. A.; Doostdar, N.; Kumar, M. K.; Barron, A. R.; Mavromoustakos, T.; Papadopoulos, M. G. In Silico Drug Screening Approach for the Design of Magic Bullets: A Successful Example with Anti-HIV Fullerene Derivatized Amino Acids. *J. Chem. Inf. Model.* **2009**, *49*, 1139–1143.
43. Research Highlights. Top Down Bottom Up: Strength in Numbers. *Nat. Nanotechnol.* **2009**, *4*, 401.
44. Chen, Y. Z.; Zhi, D. G. Ligand-Protein Inverse Docking and its Potential Use in the Computer Search of Protein Targets of a Small Molecule. *Proteins* **2001**, *43*, 217–226.
45. Paul, N.; Kellenberger, E.; Bret, G.; Muller, P.; Rognan, D. Recovering the True Targets of Specific Ligands by Virtual Screening of the Protein Data Bank. *Proteins* **2004**, *54*, 671–680.
46. Muller, P.; Lena, G.; Boilard, E.; Bezzine, S.; Lambeau, G.; Guichard, G.; Rognan, D. In Silico-Guided Target Identification of a Scaffold-Focused Library: 1,3,5-Triazepan-2,6-Diones as Novel Phospholipase A2 Inhibitors. *J. Med. Chem.* **2006**, *49*, 6768–6778.
47. Gao, Z.; Li, H.; Zhang, H.; Liu, X.; Kang, L.; Luo, X.; Zhu, W.; Chen, K.; Wang, X.; Jiang, H. PDTD: a Web-Accessible Protein Database for Drug Target Identification. *BMC Bioinf.* **2008**, *9*, 104.
48. Kroto, H. W.; Heath, J. R.; O'Brien, S. C.; Curl, R. F.; Smalley, R. E. C_{60}: Buckminsterfullerene. *Nature* **1985**, *318*, 162–163.
49. Nakamura, E.; Tokuyama, H.; Yamago, S.; Shiraki, T.; Sugiura, Y. Biological Activity of Water-Soluble Fullerenes. Structural Dependence of DNA Cleavage, Cytotoxicity and Enzyme Inhibitory Activities Including HIV-Protease Inhibition. *Bull. Chem. Soc. Jpn.* **1996**, *69*, 2143–2151.
50. Iwata, N.; Mukai, T.; Yamakoshi, Y. N.; Hara, S.; Yanase, T.; Shoji, M.; Endo, T.; Miyata, N. Effect of C_{60}, a Fullerene, on the Activities of Glutathione S-Transferase and Glutathion-Related Enzymes. *Fullerenes, Nanotubes, Carbon Nanostruct.* **1998**, *6*, 213–226.
51. Ueng, T.-H.; Kang, J.-J.; Wang, H.-W.; Cheng, Y.-W.; Chiang, L. Y. Suppression of Microsomal Cytochrome P450-Dependent Monooxygenases and Mitochondrial Oxidative Phosphorylation by Fullerenol, a Polyhydroxylated Fullerene C_{60}. *Toxicol. Lett.* **1997**, *93*, 29–37.
52. Simic-Krstic, J. Effects of $C_{60}(OH)_{24}$ on Microtubule Assembly. *Arch. Oncol.* **1997**, *5*, 143–147.
53. Wolff, D. J.; Mialkowski, K.; Richardson, C. F.; Wilson, S. R. C_{60}-Fullerene Monomalonate Adducts Selectively Inactivate Neuronal Nitric Oxide Synthase by Uncoupling the Formation of Reactive Oxygen Intermediates from Nitric Oxide Production. *Biochemistry* **2001**, *40*, 37–45.
54. Belgorodsky, B.; Fadeev, L.; Kolsenik, J.; Gozin, M. Formation of a Soluble Stable Complex between Pristine C_{60}-Fullerene and a Native Blood Protein. *ChemBioChem* **2006**, *7*, 1783–1789.
55. Mashino, T.; Shimotohno, K.; Ikegami, N.; Nishikawa, D.; Okuda, K.; Takahashi, K.; Nakamura, S.; Mochizuki, M. Human Immunodeficiency Virus-Reverse Transcriptase Inhibition and Hepatitis C Virus RNA-Dependent RNA Polymerase Inhibition Activities of Fullerene Derivatives. *Bioorg. Med. Chem. Lett.* **2005**, *15*, 1107–1109.
56. Pastorin, G.; Marchesan, S.; Hoebeke, J.; Da Ros, T.; Ehret-Sabatier, L.; Briand, J.-P.; Prato, M.; Bianco, A. Design and Activity of Cationic Fullerene Derivatives as Inhibitors of Acetylcholinesterase. *Org. Biomol. Chem.* **2006**, *4*, 2556–2562.
57. Ryan, J. J.; Bateman, H. R.; Stover, A.; Gomez, G.; Norton, S. K.; Zhao, W.; Schwartz, L. B.; Lenk, R.; Kepley, C. L. Fullerene Nanomaterials Inhibit the Allergic Response. *J. Immunol* **2007**, *179*, 665–672.
58. Cai, J.; Han, C.; Hu, T.; Zhang, J.; Wu, D.; Wang, F.; Liu, Y.; Ding, J.; Chen, K.; Yue, J.; Shen, X.; Jiang, H. Peptide Deformylase is a Potential Target for Anti-Helicobacter Pylori Drugs: Reverse Docking, Enzymatic Assay, and X-ray Crystallography Validation. *Protein Sci.* **2006**, *15*, 2071–2081.
59. Li, H.; Gao, Z.; Kang, L.; Zhang, H.; Yang, K.; Yu, K.; Luo, X.; Zhu, W.; Chen, K.; Shen, J.; Wang, X.; Jiang, H. TarFisDock: a Web Server for Identifying Drug Targets with Docking Approach. *Nucleic Acids Res.* **2006**, *34*, W219–224.
60. Arevalo, J. H.; Hassig, C. A.; Stura, E. A.; Sims, M. J.; Taussig, M. J.; Wilson, I. A. Structural Analysis of Antibody Specificity: Detailed Comparison of Five Fab′-Steroid Complexes. *J. Mol. Biol.* **1994**, *241*, 663–690.
61. Taylor, P. The Cholinesterases. *J. Biol. Chem.* **1991**, *266*, 4025–4028.
62. Sussman, J. L.; Harel, M.; Frolow, F.; Oefner, C.; Goldman, A.; Toker, L.; Silman, I. Atomic Structure of Acetylcholinesterase from Torpedo Californica: a Prototypic Acetylcholine-Binding Protein. *Science* **1991**, *253*, 872–879.
63. Axelsen, P. H.; Harel, M.; Silman, I.; Sussman, J. L. Structure and Dynamics of the Active Site Gorge of Acetylcholinesterase: Synergistic Use of Molecular Dynamics Simulation and X-ray Crystallography. *Protein Sci.* **1994**, *3*, 188–197.
64. Harel, M.; Schalk, I.; Ehret-Sabatier, L.; Bouet, F.; Goeldner, M.; Hirth, C.; Axelsen, P. H.; Silman, I.; Sussman, J. L. Quaternary Ligand Binding to Aromatic Residues in the Active-Site Gorge of Acetylcholinesterase. *Proc. Natl. Acad. Sci. U.S.A* **1993**, *90*, 9031–9035.
65. Li, Y.; Love, M. L.; Putkey, J. A.; Cohen, C. Bepridil Opens the Regulatory N-Terminal Lobe of Cardiac Troponin *C*. *Proc. Natl. Acad. Sci. U.S.A* **2000**, *97*, 5140–5145.
66. Hilge, M.; Siegal, G.; Vuister, G. W.; Guentert, P.; Gloor, S. M.; Abrahams, J. P. ATP-Induced Conformational Changes of the Nucleotide-Binding Domain of Na, K-ATPase. *Nat. Struct. Biol.* **2003**, *10*, 468–474.
67. Abrahams, J. P.; Buchanan, S. K.; Van Raaij, M. J.; Fearnley, I. M.; Leslie, A. G.; Walker, J. E. The Structure of Bovine F1-ATPase Complexed with the Peptide Antibiotic Efrapeptin. *Proc. Natl. Acad. Sci. U.S.A* **1996**, *93*, 9420–9424.
68. Kozielski, F.; De Bonis, S.; Burmeister, W. P.; Cohen-Addad, C.; Wade, R. H. The Crystal Structure of the Minus-End-Directed Microtubule Motor Protein ncd Reveals Variable Dimer Conformations. *Structure* **1999**, *7*, 1407–1416.
69. Matthews, J. H.; Krishnan, R.; Costanzo, M. J.; Maryanoff, B. E.; Tulinsky, A. Crystal Structures of Thrombin with Thiazole-Containing Inhibitors: Probes of the S1′ Binding Site. *Biophys. J.* **1996**, *71*, 2830–2839.
70. Das, K.; Ding, J.; Hsiou, Y.; Clark Jr., A. D.; Moereels, H.; Koymans, L.; Andries, K.; Pauwels, R.; Janssen, P. A.; Boyer, P. L.; et al. Crystal Structures of 8-Cl and 9-Cl TIBO Complexed with Wild-Type HIV-1 RT and 8-Cl TIBO Complexed with the Tyr181Cys HIV-1 RT Drug-Resistant Mutant. *J. Mol. Biol.* **1996**, *264*, 1085–1100.
71. Kohlstaedt, L. A.; Wang, J.; Friedman, J. M.; Rice, P. A.; Steitz, T. A. Crystal Structure at 3.5 Å Resolution of HIV-1 Reverse Transcriptase Complexed with an Inhibitor. *Science* **1992**, *256*, 1783–1790.
72. Benyamini, H.; Shulman-Peleg, A.; Wolfson, H. J.;

Belgorodsky, B.; Fadeev, L.; Gozin, M. Interaction of C_{60}-Fullerene and Carboxyfullerene with Proteins: Docking and Binding Site Alignment. *Bioconjugate Chem.* **2006**, *17*, 378–386.
73. Norman, A. W.; Mizwicki, M. T.; Norman, D. P. G. Steroid-Hormone Rapid Actions, Membrane Receptors and a Conformational Ensemble Model. *Nat. Rev. Drug Discovery* **2004**, *3*, 27–41.
74. Schimmer, B. P.; Parker, K. L. Adrenocorticotropic Hormone. Adrenocortical Steroids and Their Synthetic Analogues: Inhibitors of the Synthesis and Actions of Adrenocortical Hormones. In *Goodman and Gilman's The Pharmacological Basis of Therapeutics*, 10th ed.; Hardman, J. G., Limbird, L. E., Gilman, A. G., Eds.; McGraw-Hill: New York, 2001; pp 1649−1677.
75. Buttgereit, F.; Straub, R. H.; Wehling, M.; Burmester, G.-R. Glucocorticoids in the Treatment of Rheumatic Diseases: An Update on the Mechanisms of Action. *Arthritis Rheum.* **2004**, *50*, 3408–3417.
76. Schacke, H.; Docke, W. D.; Asdullah, K. Mechanisms Involved in the Side Effects of Glucocorticoids. *Pharmacol. Ther.* **2002**, *96*, 23–43.
77. Shu, Q.; Nair, V. Inosine Monophosphate Dehydrogenase (IMPDH) as a Target in Drug Discovery. *Med. Chem. Rev.* **2008**, *28*, 219–232.
78. Chen, L.; Pankiewicz, K. W. Recent Development of IMP Dehydrogenase Inhibitors for the Treatment of Cancer. *Curr. Opin. Drug Discovery Dev.* **2007**, *10*, 403–412.
79. Nair, V.; Shu, Q. Inosine Monophosphate Dehydrogenase as a Probe in Antiviral Drug Discovery. *Antiviral Chem. Chemother.* **2007**, *18*, 245–258.
80. Ratcliffe, A. J. Inosine 5′-Monophosphate Dehydrogenase Inhibitors for the Treatment of Autoimmune Diseases. *Curr. Opin. Drug Discovery Dev.* **2006**, *9*, 595–605.
81. Hawser, S.; Lociuro, S.; Islam, K. Dihydrofolate Reductase Inhibitors as Antibacterial Agents. *Biochem. Pharmacol.* **2006**, *71*, 941–948.
82. Gmeiner, H. W. Novel Chemical Strategies for Thymidylate Synthase Inhibition. *Curr. Med. Chem.* **2005**, *12*, 191–202.
83. Gangjee, A.; Kurup, S.; Namjoshi, O. Dihydrofolate Reductase as a Target for Chemotherapy in Parasites. *Curr. Pharm. Des.* **2007**, *13*, 609–639.
84. Berman, E. M.; Werbel, L. M. The Renewed Potential for Folate Antagonists in Contemporary Cancer Chemotherapy. *J. Med. Chem.* **1991**, *34*, 479–485.
85. Talukdar, A.; Breen, M.; Bacher, A.; Illarionov, B.; Fischer, M.; Georg, G.; Ye, Q.-Z.; Cushman, M. Discovery and Development of a Small Molecule Library with Lumazine Synthase Inhibitory Activity. *J. Org. Chem.* **2009**, *74*, 5123–5134.
86. Shoukry, K.; Schulz, H. Significance of the Reductase-Dependent Pathway for the β-Oxidation of Unsaturated Fatty Acids with Odd-Numbered Double Bonds: Mitochondrial Metabolism of 2-*trans*-5-*cis*-Octadienoyl-CoA. *J. Biol. Chem.* **1998**, *273*, 6892–6899.
87. Nelson, G. Dietary Fat, Trans Fatty Acids and Risk of Coronary Heart Disease. *Nutr. Rev.* **1998**, *56*, 250–252.
88. Ip, C.; Marshall, J. Trans Fatty Acids and Cancer. *Nutr. Rev.* **1996**, *54*, 138–145.
89. Salmeron, J.; Hu, F.; Manson, J.; Stampfer, M. Dietary Fat Intake and Risk of Type 2 Diabetes in Women. *Am. J. Clin. Nutr.* **2001**, *73*, 1019–1026.
90. Bell, P.; Cheon, S.; Fillers, S.; Foley, J.; Fraser, J.; Smith, H.; Young, D.; Revesz, L. Design of Novel Agents for the Therapy of Non-Insulin-Dependent Diabetes Mellitus (NIDDM). *Bioorg. Med. Chem. Lett.* **1993**, *3*, 1007–1012.
91. MacKenzie, R. E. Biogenesis and Interconversion of Substituted Tetrahydrofolates. In *Folates and Pterins Chemistry and Biochemistry*; Blakley, R. L., Benkovic, S. J., Eds.; Wiley: New York, 1984; Vol. I, pp 255−306.
92. Rosowsky, A. Chemistry and Biological Activity of Antifolates. In *Progress in Medicinal Chemistry*; Ellis, G. P., West, G. B., Eds.; Elsevier Science Publishers:: Amsterdam, 1989; pp 1−252.
93. Gangjee, A.; Elzein, E.; Kothare, M.; Vasudevan, A. Classical and Nonclassical Antifolates as Potential Antitumor, Antipneumocystis, and Antitoxoplasma Agents. *Curr. Pharm. Des.* **1996**, *2*, 263–280.
94. Gangjee, A.; Devraj, R.; McGuire, J. J.; Kisliuk, R. L. 5-Arylthio Substituted 2-Amino-4-oxo-6-methylpyrrolo[2,3-*d*]pyrimidine Antifolates as Thymidylate Synthase Inhibitors and Antitumor Agents. *J. Med. Chem.* **1995**, *38*, 4495–4502.
95. Gangjee, A.; Jain, H. D.; McGuire, J. J.; Kisliuk, R. L. Benzoyl Ring Halogenated Classical 2-Amino-6-methyl-3,4-dihydro-4-oxo-5-substituted Thiobenzoyl-7*H*-pyrrolo[2,3-*d*]pyrimidine Antifolates as Inhibitors of Thymidylate Synthase and as Antitumor Agents. *J. Med. Chem.* **2004**, *47*, 6730–6739.
96. Gangjee, A.; Qiu, Y.; Li, W.; Kisliuk, R. L. Potent Dual Thymidylate Synthase and Dihydrofolate Reductase Inhibitors: Classical and Nonclassical 2-Amino-4-oxo-5-arylthio-substituted-6-methylthieno[2,3-*d*]pyrimidine Antifolates. *J. Med. Chem.* **2008**, *51*, 5789–5797.
97. Gangjee, A.; Li, W.; Kisliuk, R. L.; Cody, V.; Pace, J.; Piraino, J.; Makin, J. Design, Synthesis, and X-ray Crystal Structure of Classical and Nonclassical 2-Amino-4-oxo-5-substituted-6-ethylthieno[2,3-*d*]pyrimidines as Dual Thymidylate Synthase and Dihydrofolate Reductase Inhibitors and as Potential Antitumor Agents. *J. Med. Chem.* **2009**, *52*, 4892–4902.
98. Cao, W.; Matherly, L. H. Structural Determinants of Folate and Antifolate Membrane Transport by the Reduced Folate Carrier. In *Drug Metabolism and Transport*; Lash, L. H., Ed.; Humana Press: Totowa, NJ, 2005; pp 291−318.
99. Assaraf, Y. G. Molecular Basis of Antifolate Resistance. *Cancer Metastasis Rev.* **2007**, *26*, 153–181.
100. Matherly, L. H.; Hou, Z. Structure and Function of the Reduced Folate Carrier a Paradigm of a Major Facilitator Superfamily Mammalian Nutrient Transporter. *Vitam. Horm.* **2008**, *79*, 145–184.
101. Wong, S. C.; Zhang, L.; Witt, T. L.; Proefke, S. A.; Bhushan, A.; Matherly, L. H. Impaired Membrane Transport in Methotrexate-resistant CCRF-CEM Cells Involves Early Translation Termination and Increased Turnover of a Mutant Reduced Folate Carrier. *J. Biol. Chem.* **1999**, *274*, 10388–10394.
102. Chawla, A.; Repa, J. J.; Evans, R. M.; Mangelsdorf, D. J. Nuclear Receptors and Lipid Physiology: Opening the X-Files. *Science* **2001**, *294*, 1866–1870.
103. Staudinger, J. L.; Goodwin, B.; Jones, S. A.; Hawkins-Brown, D.; MacKenzie, K. I.; LaTour, A.; Liu, Y.; Klaassen, C. D.; Brown, K. K.; Reinhard, J.; et al. The Nuclear Receptor PXR is a Lithocholic Acid Sensor that Protects Against Liver Toxicity. *Proc. Natl. Acad. Sci. U.S.A* **2001**, *98*, 3369–3374.
104. Xie, W.; Radominska-Pandya, A.; Shi, Y.; Simon, C. M.; Nelson, M. C.; Ong, E. S.; Waxman, D. J.; Evans, R. M. An Essential Role for Nuclear Receptors SXR/PXR in Detoxification of Cholestatic Bile Acids. *Proc. Natl. Acad. Sci. U.S.A* **2001**, *98*, 3375–3380.
105. Zhai, Y.; Pai, H. V.; Zhou, J.; Amico, J. A.; Vollmer, R. R.; Xie, W. Activation of Pregnane X Receptor Disrupts Glucocorticoid and Mineralocorticoid Homeostasis. *Mol. Endocrinol.* **2007**, *21*, 138–147.
106. Handschin, C.; Meyer, U. A. Regulatory Network of Lipid-Sensing Nuclear Receptors: Roles for CAR, PXR, LXR, and FXR. *Arch. Biochem. Biophys.* **2005**, *433*, 387–396.
107. Dring, M. M.; Goulding, C. A.; Trimble, V. I.; Keegan, D.; Ryan, A. W.; Brophy, K. M.; Smyth, C. M.; Keeling, P. W.; O'Donoghue, D.; O'Sullivan, M.; et al. The Pregnane X Receptor Locus is Associated with Susceptibility to Inflammatory Bowel Disease. *Gastroenterology* **2006**, *130*, 341–348.
108. Shah, Y. M.; Ma, X.; Morimura, K.; Kim, I.; Gonzalez, F. J. Pregnane X Receptor Activation Ameliorates DSS-Induced Inflammatory Bowel Disease *via* Inhibition of NF-κB Target Gene Expression. *Am. J. Physiol. Gastrointest. Liver Physiol* **2007**, *292*, G1114–G1122.

109. Pascussi, J. M.; Robert, A.; Nguyen, M.; Walrant-Debray, O.; Garabedian, M.; Martin, P.; Pineau, T.; Saric, J.; Navarro, F.; Maurel, P.; et al. Possible Involvement of Pregnane X Receptor-Enhanced CYP24 Expression in Drug-Induced Osteomalacia. *Clin. Invest.* **2005**, *115*, 177–186.
110. Zhang, B.; Xie, W.; Krasowski, M. D. PXR: a Xenobiotic Receptor of Diverse Function Implicated in Pharmacogenetics. *Pharmacogenomics* **2008**, *9*, 1695–1709.
111. Gupta, D.; Venkatesh, M. K.; Wang, H.; Kim, S.; Sinz, M.; Goldberg, G. L.; Whitney, K.; Mani, S. Expanding the Roles for Pregnane X Receptor in Cancer: Proliferation and Drug Resistance in Ovarian Cancer. *Clin. Cancer Res.* **2008**, *14*, 5332–5340.
112. Wang, H.; Huang, H.; Li, H.; Teotico, D. G.; Sinz, M.; Baker, S. D.; Staudinger, J.; Kalpana, G.; Redinbo, M. R.; Mani, S. Activated Pregnenolone X-Receptor Is a Target for Ketoconazole and Its Analogs. *Clin. Cancer Res.* **2007**, *13*, 2488–2495.
113. Zhou, C.; Poulton, E. J.; Grun, F.; Bammler, T. K.; Blumberg, B.; Thummel, K. E.; Eaton, D. L. The Dietary Isothiocyanate Sulforaphane Is an Antagonist of the Human Steroid and Xenobiotic Nuclear Receptor. *Mol. Pharmacol.* **2007**, *71*, 220–229.
114. Synold, T. W.; Dussault, I.; Forman, B. M. The Orphan Nuclear Receptor SXR Coordinately Regulates Drug Metabolism and Efflux. *Nat. Med.* **2001**, *7*, 584–590.
115. Das, B. C.; Madhukumar, A. V.; Anguiano, J.; Kim, S.; Sinz, M.; Zvyaga, T. A.; Power, E. C.; Ganellin, C. B.; Mani, S. Synthesis of Novel Ketoconazole Derivatives as Inhibitors of the Human Pregnane X Receptor (PXR; NR1I2; also Termed SXR, PAR). *Bioorg. Med. Chem. Lett.* **2008**, *18*, 3974–3977.
116. Penning, T. M.; Bennett, M. J.; Smith-Hoog, S.; Schlegel, B. P.; Jez, J. M.; Lewis, M. Structure and Function of 3-Alpha-Hydroxysteroid Dehydrogenase. *Steroids* **1997**, *62*, 101–111.
117. Fairlamb, A. H.; Blackburn, P.; Ulrich, P.; Chait, B. T.; Cerami, A. Trypanothione: a Novel Bis(glutathionyl)spermidine Cofactor for Glutathione Reductase in Trypanosomatids. *Science* **1985**, *227*, 1485–1487.
118. Liu, G.; Lin, Y. Biosensor Based on Self-Assembling Acetylcholinesterase on Carbon Nanotubes for Flow Injection/Amperometric Detection of Organophosphate Pesticides and Nerve Agents. *Anal. Chem.* **2006**, *78*, 835–843.
119. Li, G.; Liao, J. M.; Hu, G. Q.; Ma, N. Z.; Wu, P. J. Study of Carbon Nanotube Modified Biosensor for Monitoring Total Cholesterol in Blood. *Biosens. Bioelectron.* **2005**, *20*, 2140–2144.
120. Carrara, S.; Shumyantseva, V. V.; Archakov, A. I.; Samorì, B. Screen-Printed Electrodes Based on Carbon Nanotubes and Cytochrome P450scc for Highly-Sensitive Cholesterol. *Biosens. Bioelectron.* **2008**, *24*, 148–150.
121. Sanchez-Acevedo, Z. C.; Riu, J.; Rius, F. X. Fast Picomolar Selective Detection of Bisphenol A in Water Using a Carbon Nanotube Field Effect Transistor Functionalized with Estrogen Receptor-α. *Biosens. Bioelectron.* **2009**, *24*, 2842–2846.
122. Salimi, A.; Compton, R. G.; Hallaj, R. Glucose Biosensor Prepared by Glucose Oxidase Encapsulated Sol-Gel and Carbon-Nanotube-Modified Basal Plane Pyrolytic Graphite Electrode. *Anal. Biochem.* **2004**, *333*, 49–56.
123. Liu, S.; Cai, C. Immobilization and Characterization of Alcohol Dehydrogenase on Single-Walled Carbon Nanotubes and its Application in Sensing Ethanol. *J. Electroanal. Chem.* **2007**, *602*, 103–114.
124. Carano, M.; Cosnier, S.; Kordatos, K.; Marcaccio, M.; Margotti, M.; Paolucci, F.; Prato, M.; Roffia, S. A Glutathione Amperometric Biosensor Based on an Amphiphilic Fullerene Redox Mediator Immobilised Within an Amphiphilic Polypyrrole Film. *J. Mater. Chem.* **2002**, *12*, 1996–2000.
125. Schneidman-Duhovny, D.; Inbar, Y.; Polak, V.; Shatsky, M.; Halperin, I.; Benyamini, H.; Barzilai, A.; Dror, O.; Haspel, N.; Nussinov, R.; et al. Taking Geometry to its Edge: Fast Unbound Rigid (and Hinge-Bent) Docking. *Proteins* **2003**, *52*, 107–112.
126. Zhang, C.; Vasmatzis, G.; Cornette, J. L.; DeLisi, C. Determination of Atomic Desolvation Energies from the Structures of Crystallized Proteins. *J. Mol. Biol.* **1997**, *267*, 707–726.
127. Andrusier, N.; Nussinov, R.; Wolfson, H. J. FireDock: Fast Interaction Refinement in Molecular Docking. *Proteins* **2007**, *69*, 139–159.
128. Kingsford, C. L.; Chazelle, B.; Singh, M. Solving and Analyzing Side-Chain Positioning Problems Using Linear and Integer Programming. *Bioinformatics* **2005**, *21*, 1028–1036.
129. Gray, J. J.; Moughon, S.; Wang, C.; Schueler-Furman, O.; Kuhlman, B.; Rohl, C. A.; Baker, D. Protein-Protein Docking with Simultaneous Optimization of Rigid-Body Displacement and Side-Chain Conformations. *J. Mol. Biol.* **2003**, *331*, 281–299.
130. Neria, E.; Fischer, S.; Karplus, M. Simulation of Activation Free Energies in Molecular Systems. *J. Chem. Phys.* **1996**, *105*, 1902–1921.
131. Misura, K. M.; Morozov, A. V.; Baker, D. Analysis of Anisotropic Sidechain Packing in Proteins and Application to High-Resolution Structure Prediction. *J. Mol. Biol.* **2004**, *342*, 651–664.
132. Janin, J.; Henrick, K.; Moult, J.; Eyck, L. T.; Sternberg, M. J. E.; Vajda, S.; Vakser, I.; Wodak, S. J. CAPRI: A Critical Assessment of PRedicted Interactions. *Proteins* **2003**, *52*, 2–9.